40 V, 1.5 kW BLDC motor driver inverter

REF_40VDC_1.5KW_SAW

About this document

Scope and purpose

This document describes the functionalities of the REF_40VDC_1.5KW_SAW motor drive board for 40 V battery-powered brushless DC (BLDC) motor drives – operating with trapezoidal or sensorless field-oriented control (FOC) – as used in applications such as outdoor power equipment of up to 1.5 kW. This system solution is based on the PSOC™ C3 series of MCUs operating with Infineon floating point firmware and 60 V OptiMOS™ 5 power MOSFETs.

Intended audience

This document addresses the market for high power 40 V battery-powered motor drive applications, aimed at designers wishing to provide a high-performance system solution and reduce system costs; also design engineers, applications engineers, and students.

Infineon components featured

- PSC3M5EDAFQ1 (Arm® Cortex® M33 32-bit MCU+FPU+DSP, 180 MHz, 128 kB flash, 64 kB SRAM, E-LQFP-80)
- TLS203B0EJ V33 (3.3 V Linear Voltage Regulator, PG-DSO-8-27)
- ISC015N06NM5LF2ATMA1 (OptiMOS™ 5 60 V/1.55 mΩ PG-TDSON-12)
- IQFH61N06NM5 (OptiMOS™ 5 60 V/0.61 mΩ PG-TSON)
- 6ED2742S01Q (160 V Three-phase motor control gate driver IC, 32-VQFN (5x5))
- 1EDL8011 (125 V high-side disconnect switch gate driver IC, PG-DSO-8)

V 1.0
2025-04-22

Table of contents

1 Introduction

1.1 Outdoor power equipment

Outdoor power equipment (OPE) refers to high power construction and gardening tools such as lawn mowers, leaf blowers, hedge trimmers, and chainsaws. Motor drive systems in OPE are typically required to deliver power in the 1 to 2 kW power range. Older gasoline-powered outdoor power equipment are typically bulky, heavy, noisy, and produces CO^2 emissions.

With new laws and environmental regulations being passed, this type of equipment is gradually being replaced with cordless battery powered alternatives. 24 to 40 V lithium-ion battery packs are well suited for these applications as a tradeoff between lower current and safer voltage.

The need for smaller, safer, cordless and more sustainable devices challenges the industry to optimize thermal management, battery runtime, and EMI, while handling weight and size constraints.

There are three main challenges in designing battery powered OPE:

- The first is maximizing energy output while keeping the motor drive as small and light as possible. OPE motor drives must offer efficient performance at sufficient power to support torque and speed requirements
- The second is thermal management and minimization of heat produced by electrical power conversion, which also wastes battery power. The motor drive, therefore, needs to operate with the highest possible efficiency to minimize bulky and heavy heat sinks
- The third point is safety. The OPE needs to include protection against possible faults and safe shutdown to avoid potential fire hazard and injury to the user

All of these challenges, alongside factors like robustness, reliability, and adherence to EMI standards, impose constraints that the motor drive must fulfill. Infineon's latest power products can tackle these design challenges and help achieve system optimization.

1.2 REF_40VDC_1.5KW_SAW motor drive board

This application note describes Infineon's REF_40VDC_1.5KW_SAW system solution reference board optimized for 40 V battery-powered tools operating with sensorless field-oriented control. The current design embodies the electrical driving system for PMSM and BLDC machines with sensorless operation or with Hall sensors. The default control method is sensorless FOC; however, with alternative firmware, trapezoidal or vector operation with Hall sensors is also supported.

The control method implements a vector speed-control algorithm based on the BLDC motor using pulse-width modulation (PWM) and three current shunts for phase current measurement.

The firmware is from Infineon's Motor Control Firmware Solution suite and has been developed using the floating point PSOC™ C3 Arm® Cortex® M33 MCU.

This reference board lets you evaluate the OPE motor drive system solution using the control capabilities of the MCU using the implemented control algorithm. The board includes a switch for changing the motor direction and a speed control potentiometer.

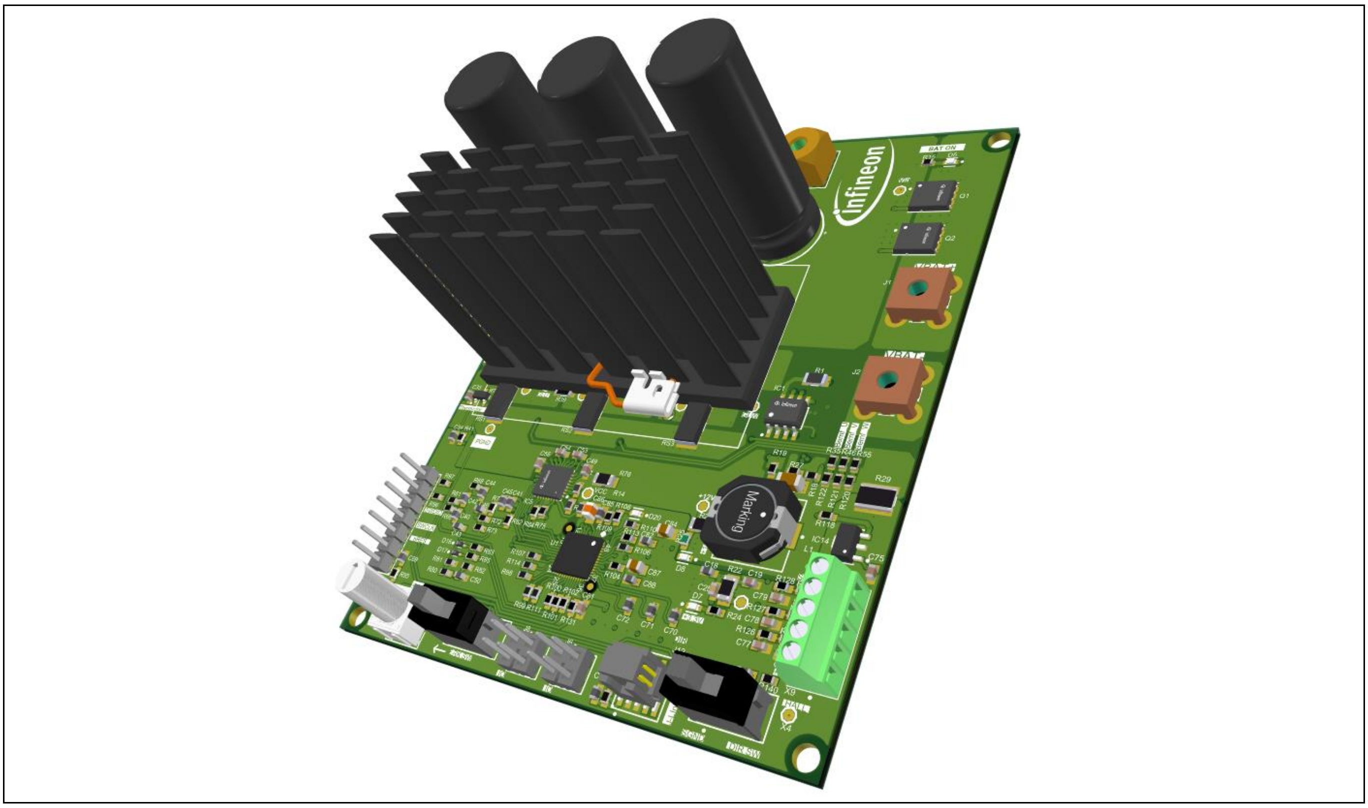

Figure 1 REF_40VDC_1.5KW_SAW reference board

The REF_40VDC_1.5KW_SAW board block diagram of the main system:

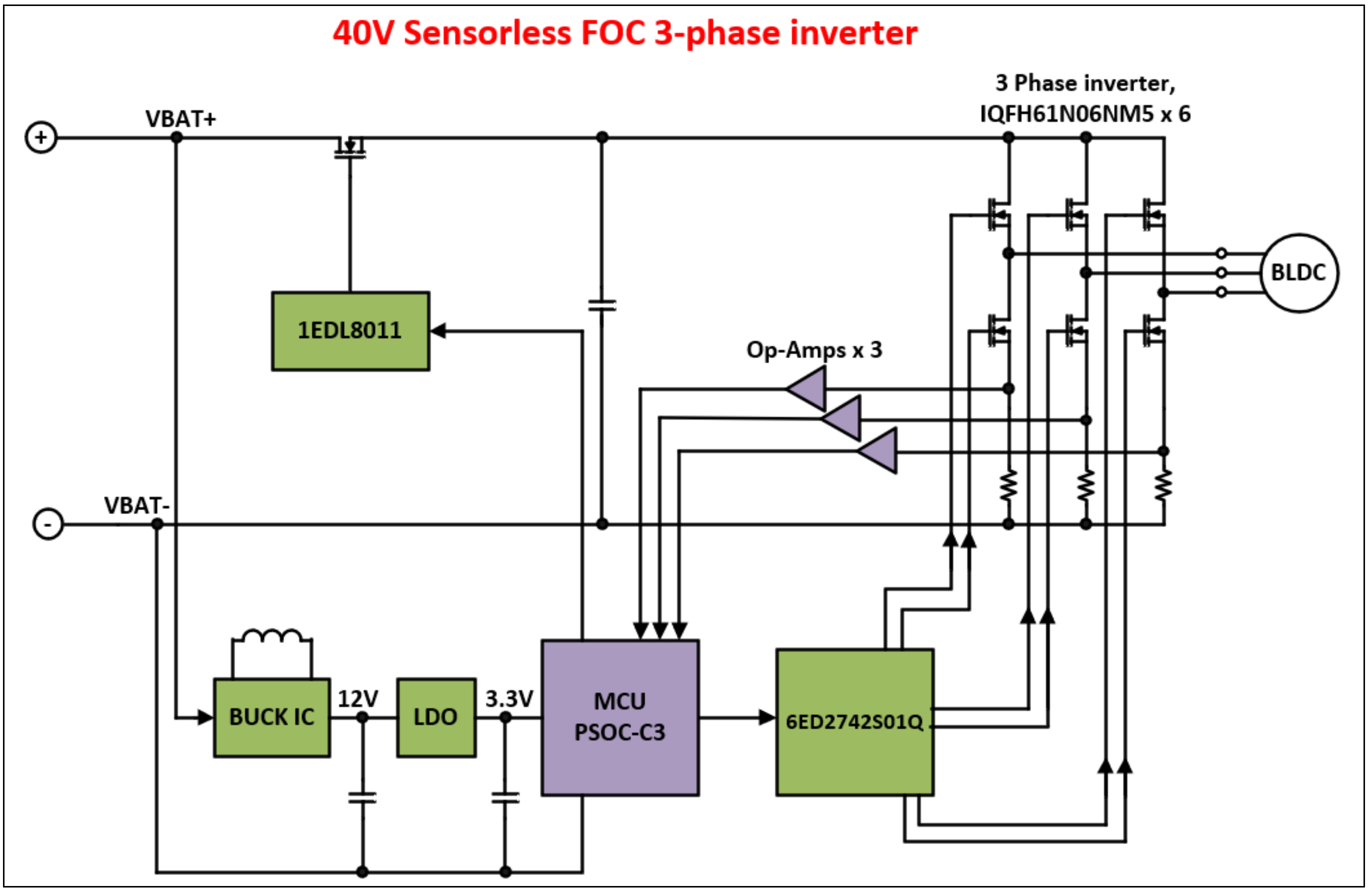

Figure 2 Simplified system block diagram

2 Specifications

Input and output in normal operation:

- DC input voltage 24 V to 40 V, nominal 36 V
- Maximum input current 42 ADC
- Output voltage three-phase trapezoidal and sensorless FOC control
- Maximum output current per phase 25 A_{rms}
- Maximum output power 1500 W for not more than one minute
- Maximum continuous output power 1000 W

Control scheme:

- Supports Trapezoidal commutation with Hall sensors and sensorless FOC
- Switching frequency 15 kHz
- Three current shunts

Protection features:

- Input overcurrent
- Phase output overcurrent
- Thermal shutdown

Maximum component temperature:

In an ambient temperature of 30°C, the maximum allowed component temperatures are:

- Resistors less than 100°C
- Ceramic capacitors, film capacitors, and electrolytic capacitors less than 100°C
- MOSFET transistors and diodes less than 100°C
- ICs less than 100°C

Dimensions of evaluation board:

- Maximum width 3.75 inches/78.6 mm, maximum length 3.82 inches/97.1 mm

3 Schematics

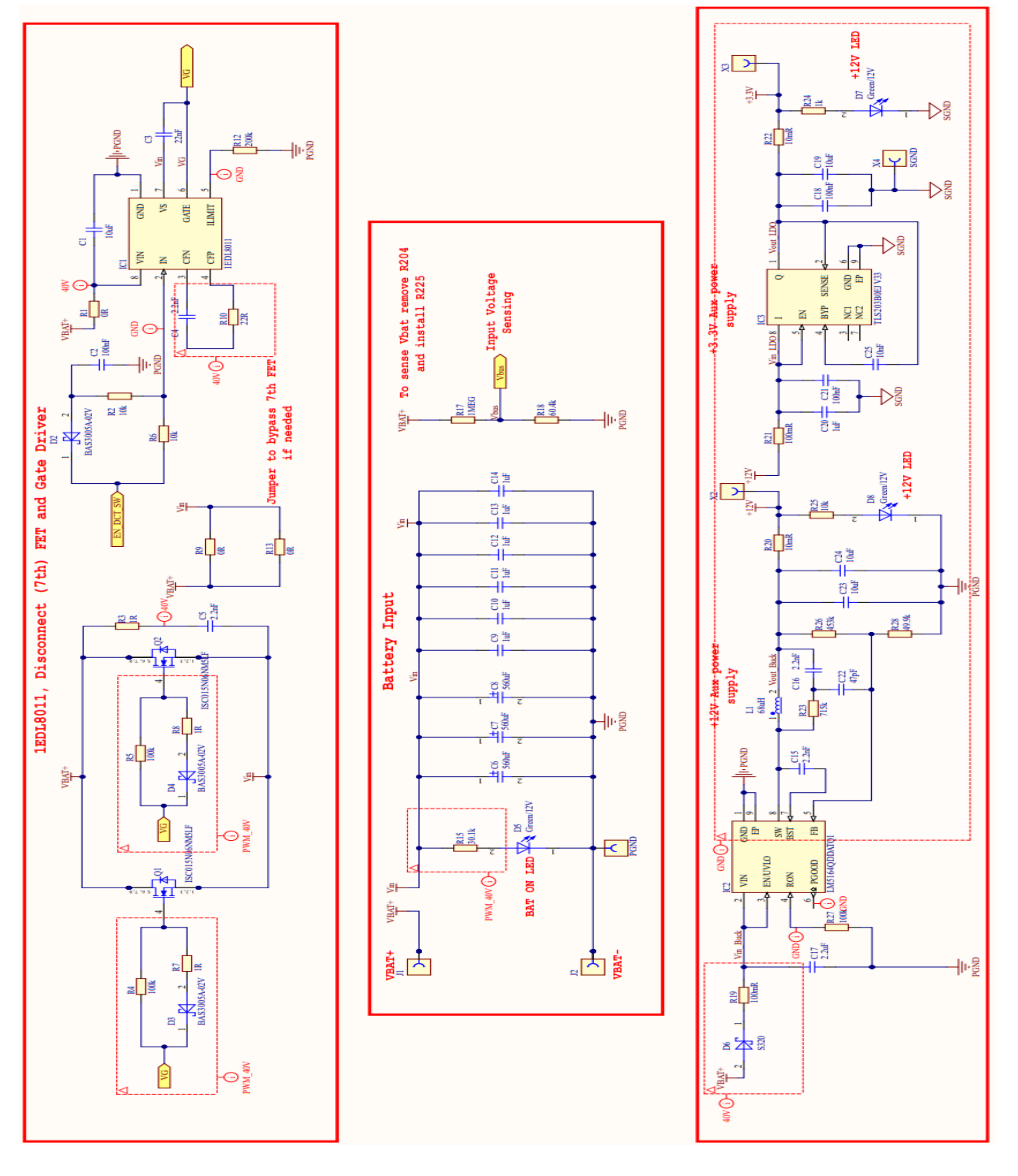

Figure 3 Input stage

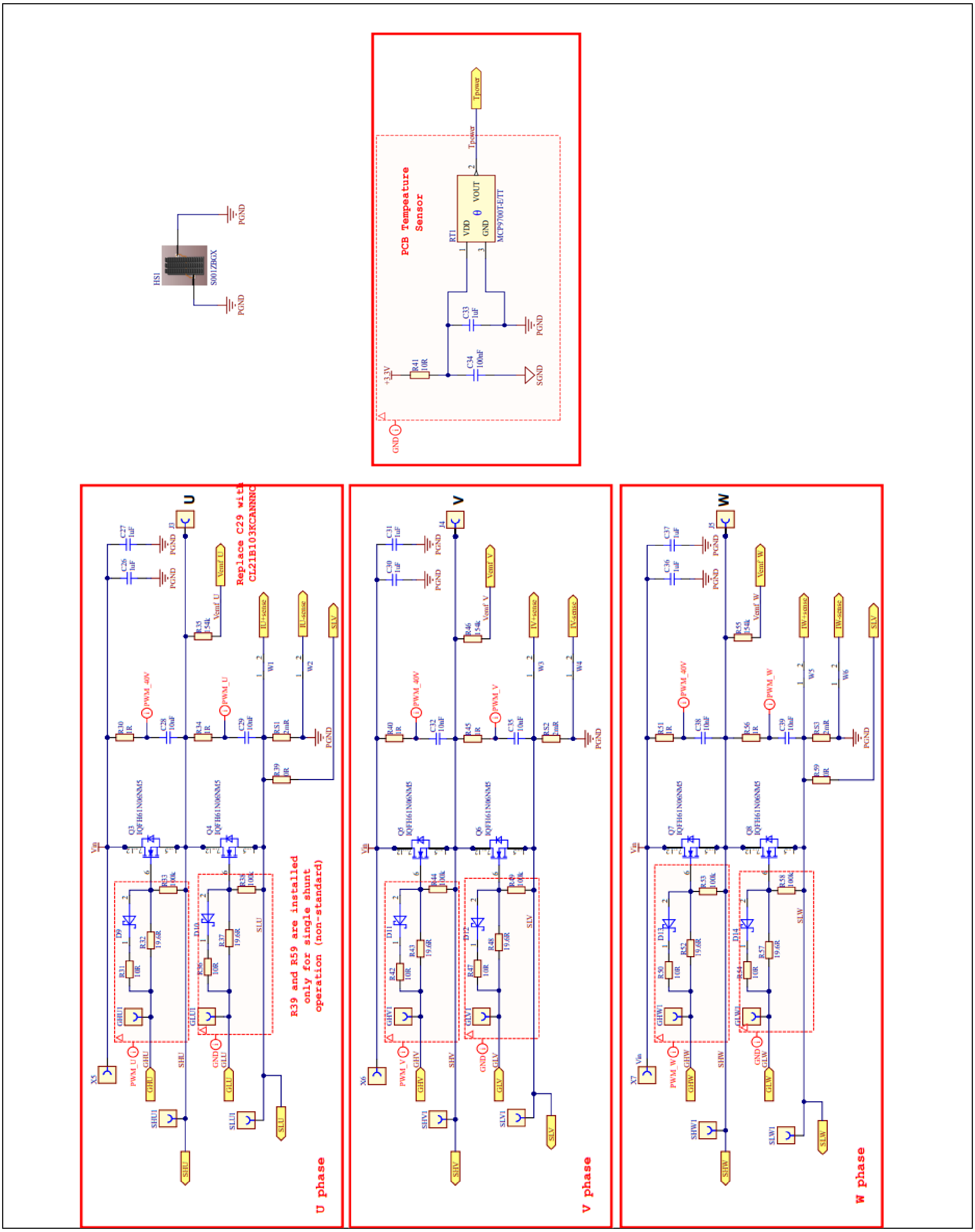

Figure 4 Power stage

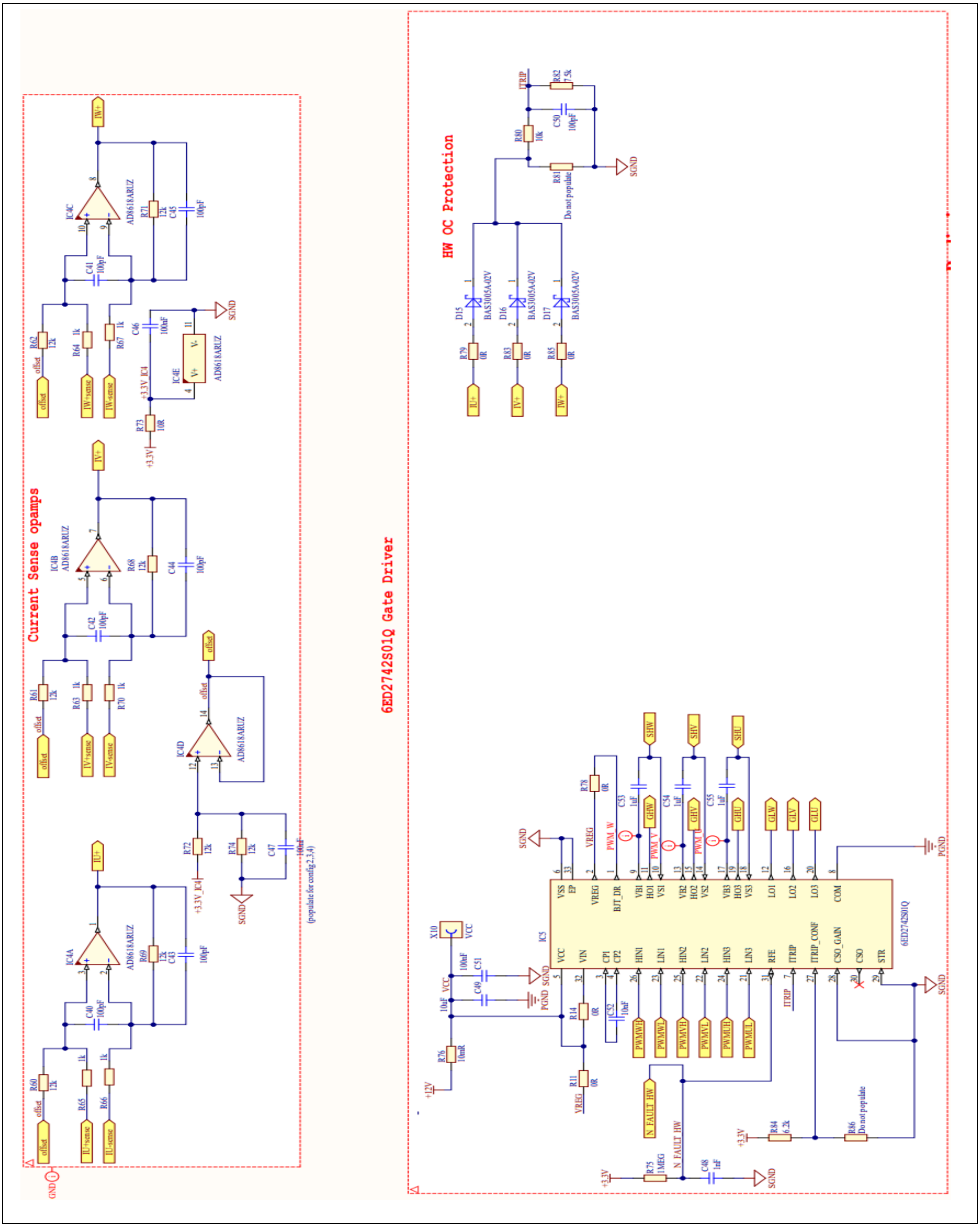

Figure 5 **Current sense and driving stage**

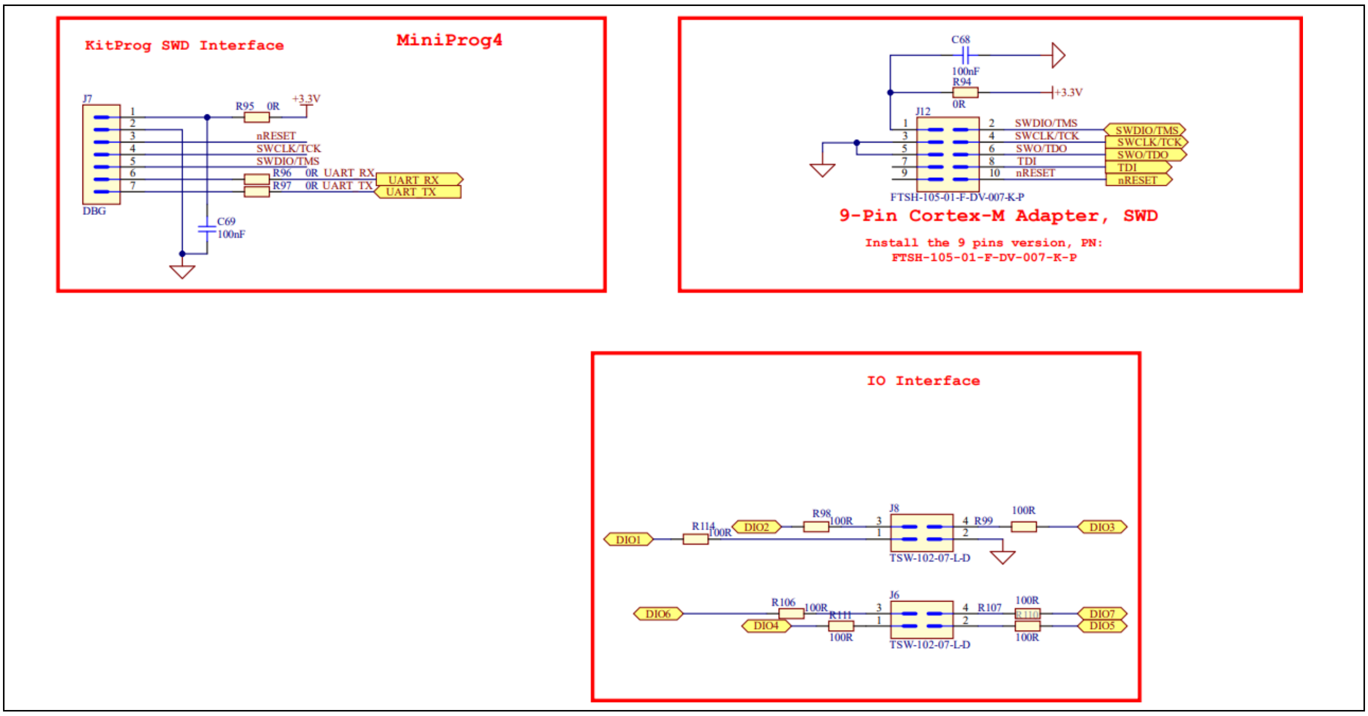

Figure 6 Board connectors

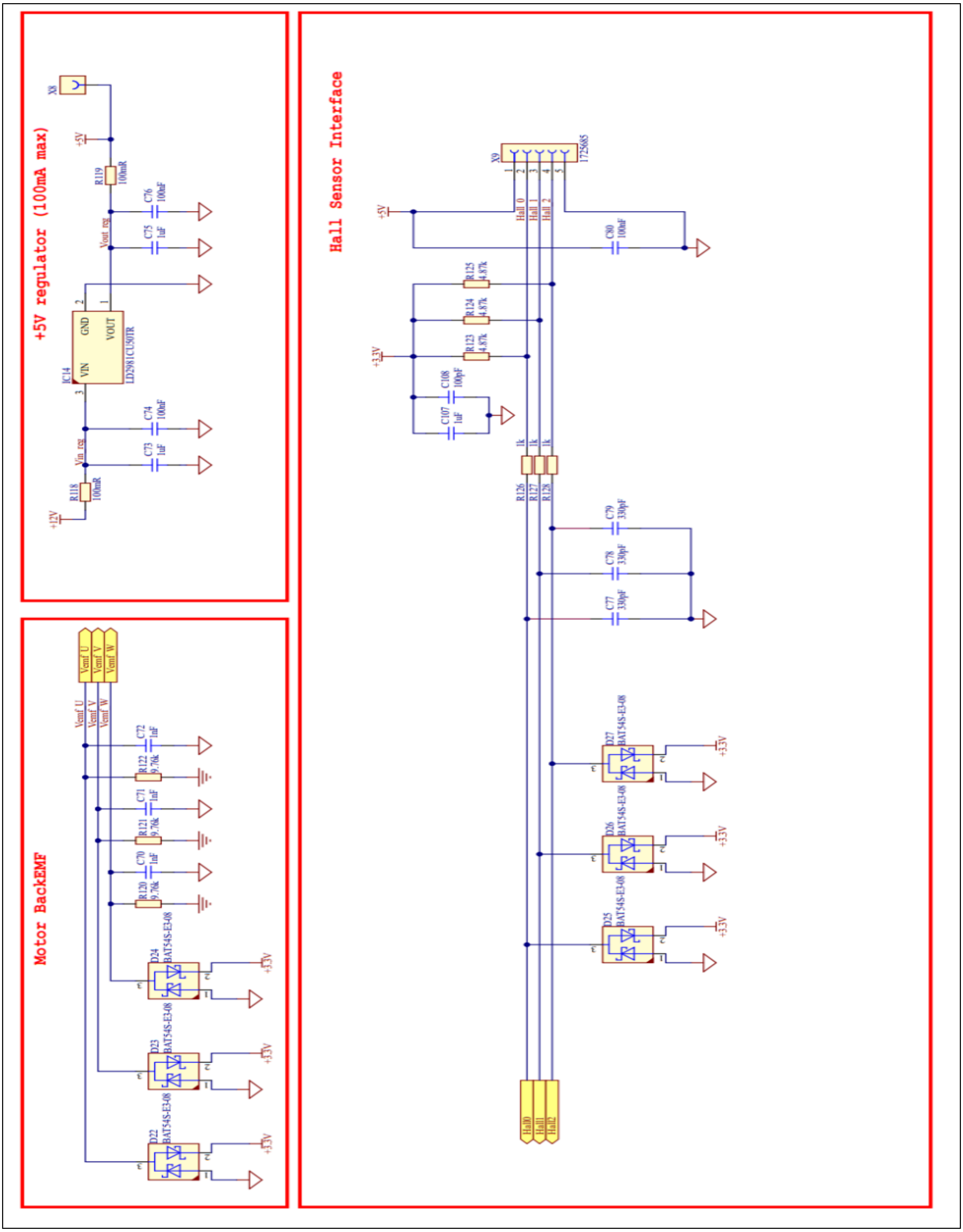

Figure 7 **POSIF connectors**

Schematics

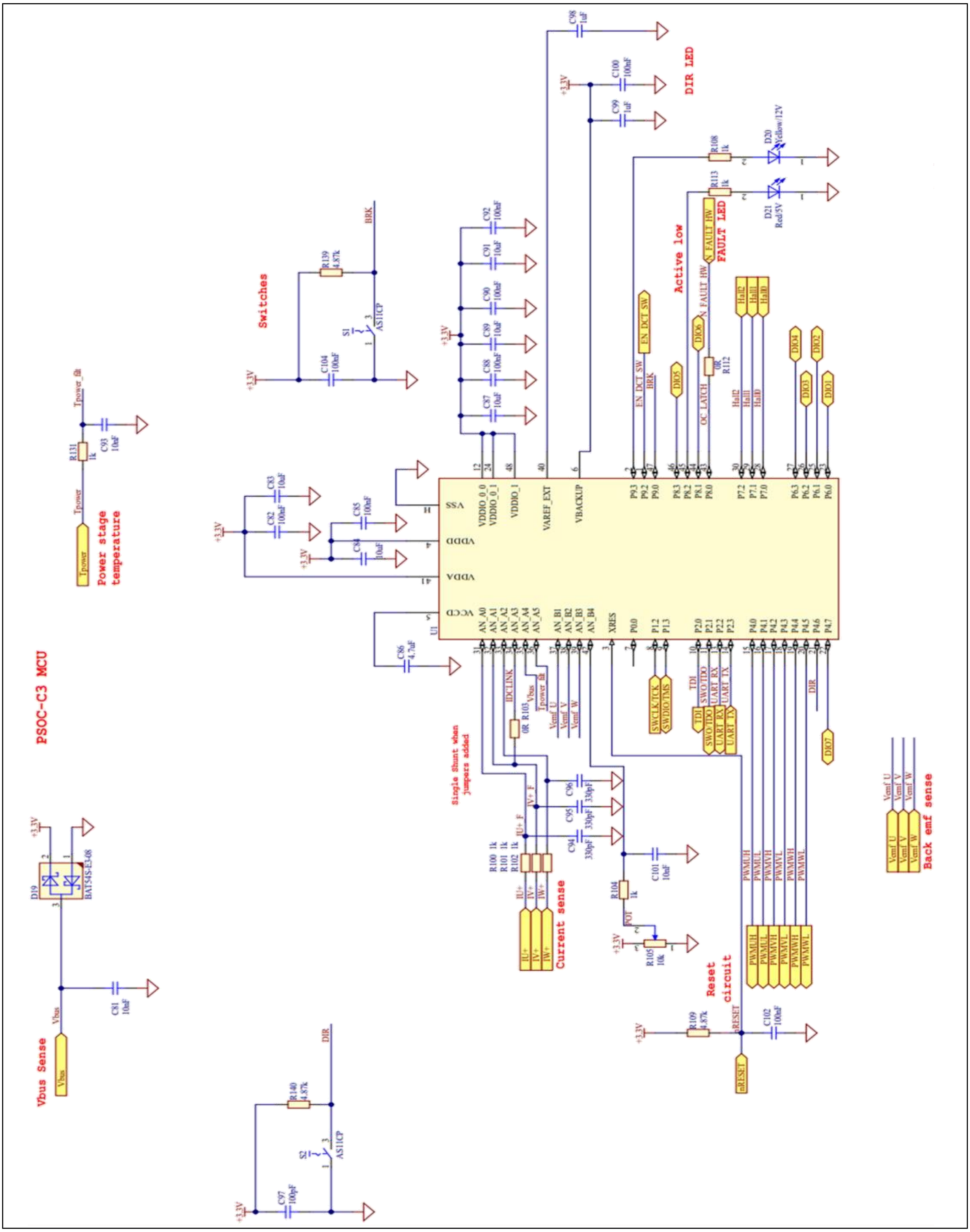

Figure 8 **Control stage**

4 Hardware functional description

The reference board consists of three half bridges that make up a three-phase inverter. Each half bridge consists of a low-side and high-side MOSFET (IQFH61N06NM5) driven by Infineon's three-phase motor control gate driver IC (6ED2742S01Q). The driver is supplied by a 40 V voltage through a buck regulator. The output of the buck regulator is then stepped down to 3.3 V by a linear voltage regulator that supplies the MCU and other ICs. The ICs on the current sensing and driving circuitry provide protection and sends signals to the MCU in the control stage.

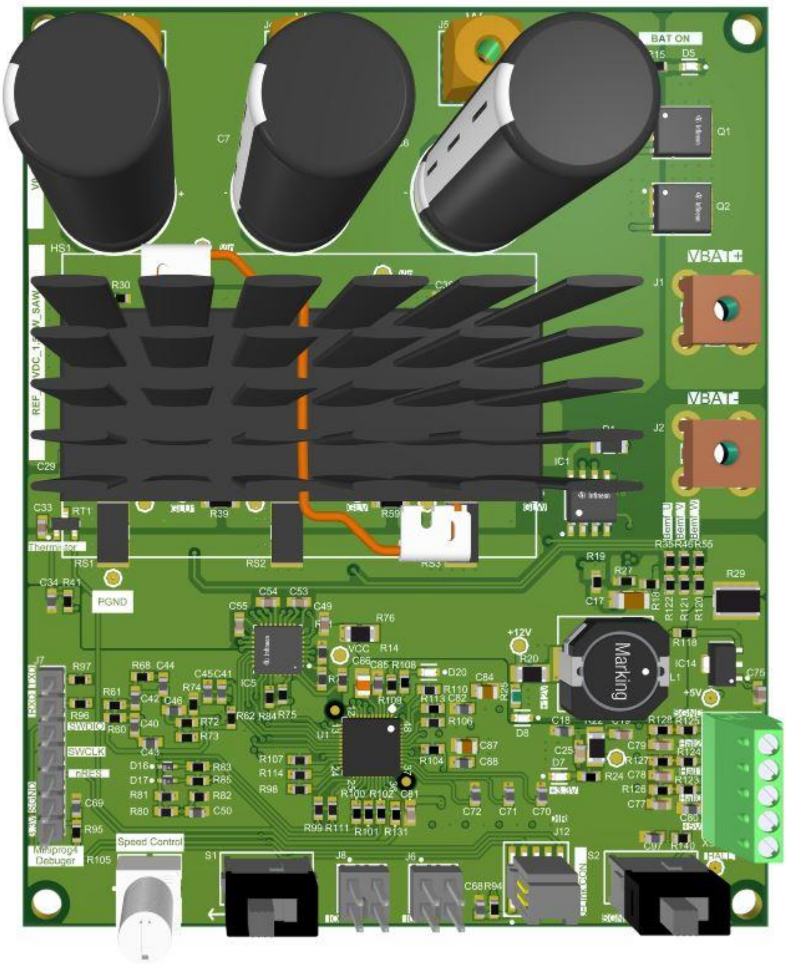

Figure 9 Input stage electrolytic capacitors and MOSFETs

The input stage is composed of two auxiliary power supplies and a three-phase half-bridge gate driver that includes protection features. When the battery voltage is enabled, 40 V is supplied to all three ICs in the input stage (Figure 10). The buck controller (IC2) is used to step down the battery voltage from 40 V to 12 V while IC3 (Infineon's TLS203B0EJ V33) is used as a second auxiliary power supply to provide 3.3 V to the MCU and other ICs.

In addition, the battery voltage is connected to Infineon's ISC015N06NM5LF2ATMA1 disconnect MOSFETs that are located at the positive input.These MOSFETs serve as safety switch to disconnect the battery voltage by Infineon's EiceDRIVER (1EDL8011) if a fault is detected. The 1EDL8011 is used to manage inrush current, disable switches with the battery supply is lower than the undervoltage lockout (UVLO) and prevent short-circuit from affecting the battery supply.

The gate of the MOSFETs turns off if one of the following conditions occur:

- The IN-pin voltage (V_IN) is less than VTHLIN (1 V maximum)
- The input voltage is less than VVIN_UVLO_F (7.5 V typical)
- OCP is triggered

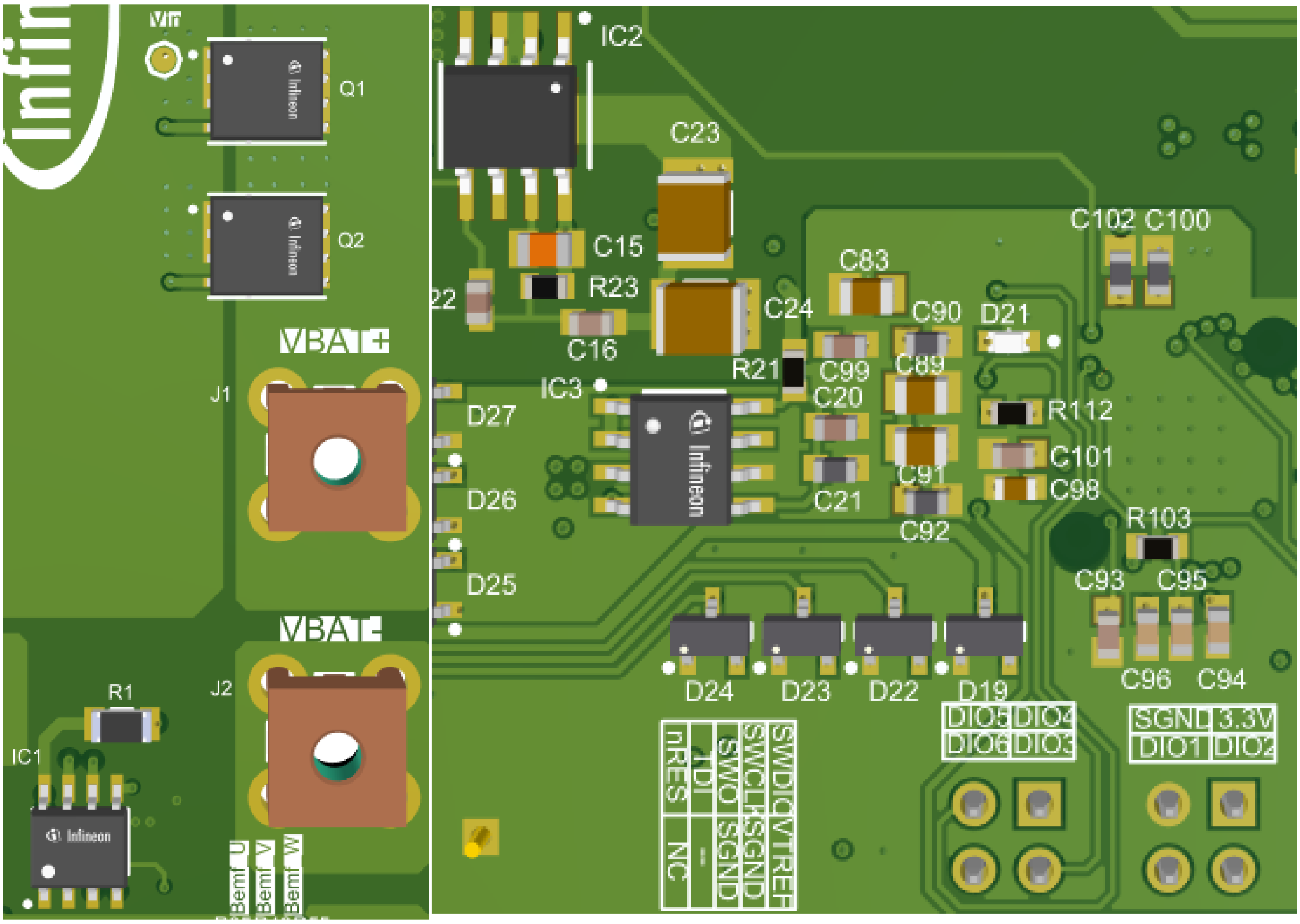

Figure 10 **Input stage ICs**

The figure below consists of three half bridges that make a three-phase inverter, along with a PCB temperature sensor (Figure 11). The input voltage from the first stage (input stage) supplies the high-side MOSFETs of each phase. Each phase uses two IQFH61N06NM5 MOSFETs optimized for battery power and low voltage drive applications. Though the package is slender in size, the IQFH61N06NM5 is robust enough to support 24 A_{RMS} per phase. In addition, 60 V rating allows enough head room for voltage spikes with low $R_{DS(on)}$ to minimize conduction loss when the MOSFETs are switched on.

A snubber is also placed in parallel with each MOSFET to suppress voltage transients. It is important to note that the efficiency of the board remains at 98% or higher with the snubbers in place. A temperature sensor is implemented in the power stage for thermal management and protection. If the board reaches over 100°C, the system goes into protection mode and shuts down.

As mentioned previously, this reference board is designed to support either single shunt or three shunt current sensing with three shunts as the default configuration. For normal current sensing operation three 1 mΩ shunts (RS1, RS2, and RS3) are located on the low side of each half bridge and ground. For single shunt current sensing, R39 and R59 can be populated with zero Ohm jumpers.

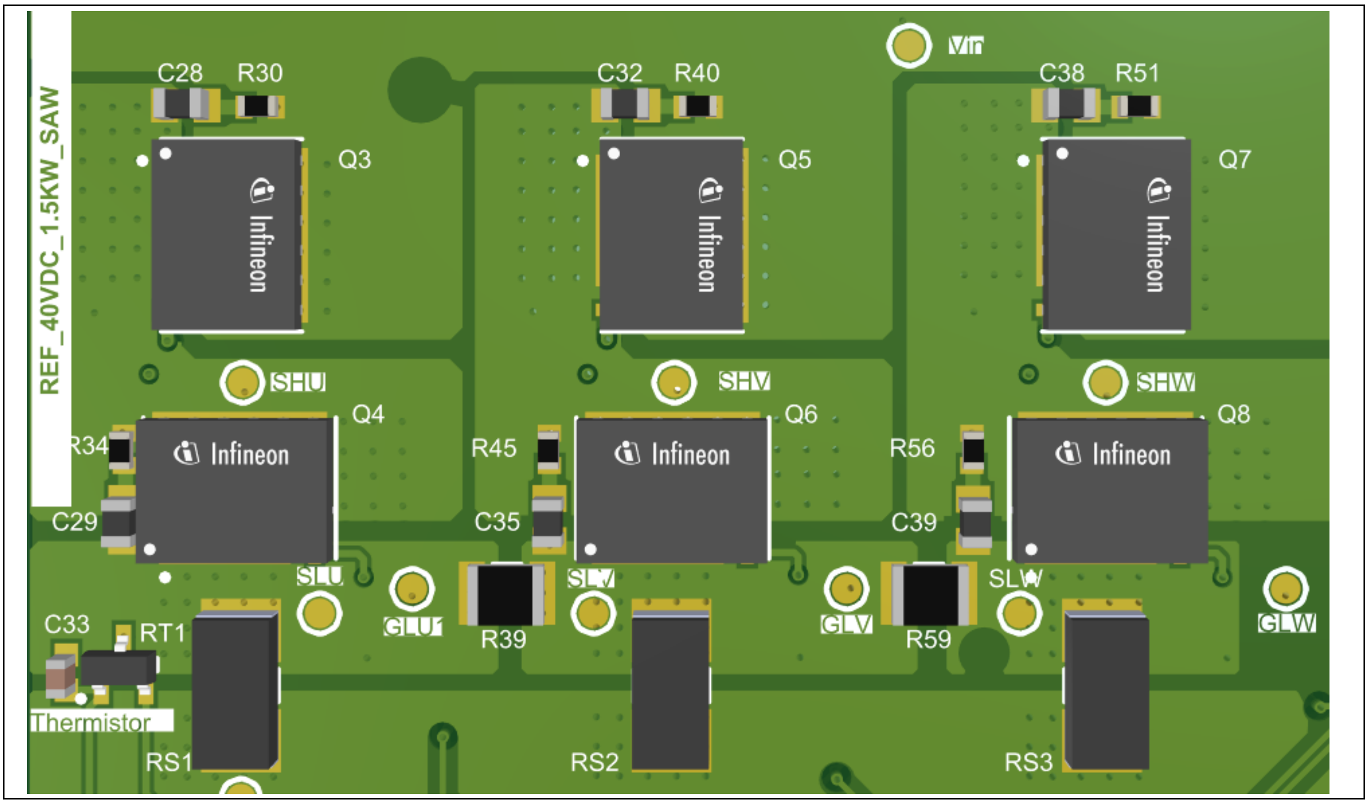

Figure 11 Power stage

An operational amplifier IC (IC4) is used to sense the output current from the shunts (RS1, RS2, and RS3) and amplify the voltage by a gain of 12. Utilizing IC4 as a differential amplifier eliminates errors due to PCB parasitics because the input voltage is differential. The amplified output is then fed into Infineon's 6ED2742S01Q gate driver (IC5), as shown on Figure 12.

The 6ED2742S01Q is a silicon-on-insulator (SOI)-based gate driver designed for three phase BLDC motor drive applications. The gate driver has a power management unit that allows the driver to operate across a wide range of input voltages without requiring an external VCC supply, however this is not used in this implementation. It includes integrated bootstrap diodes that supply the external bootstrap capacitors and supports 100% duty cycle operation using an integrated trickle charge pump. The internal trickle charge pumps supply a small current to overcome leakages that would gradually discharge the bootstrap capacitors during 100% duty cycle operation. The charge pumps are activated when the HIN/HO signal of the respective phase remains high for typically 1.8 ms.

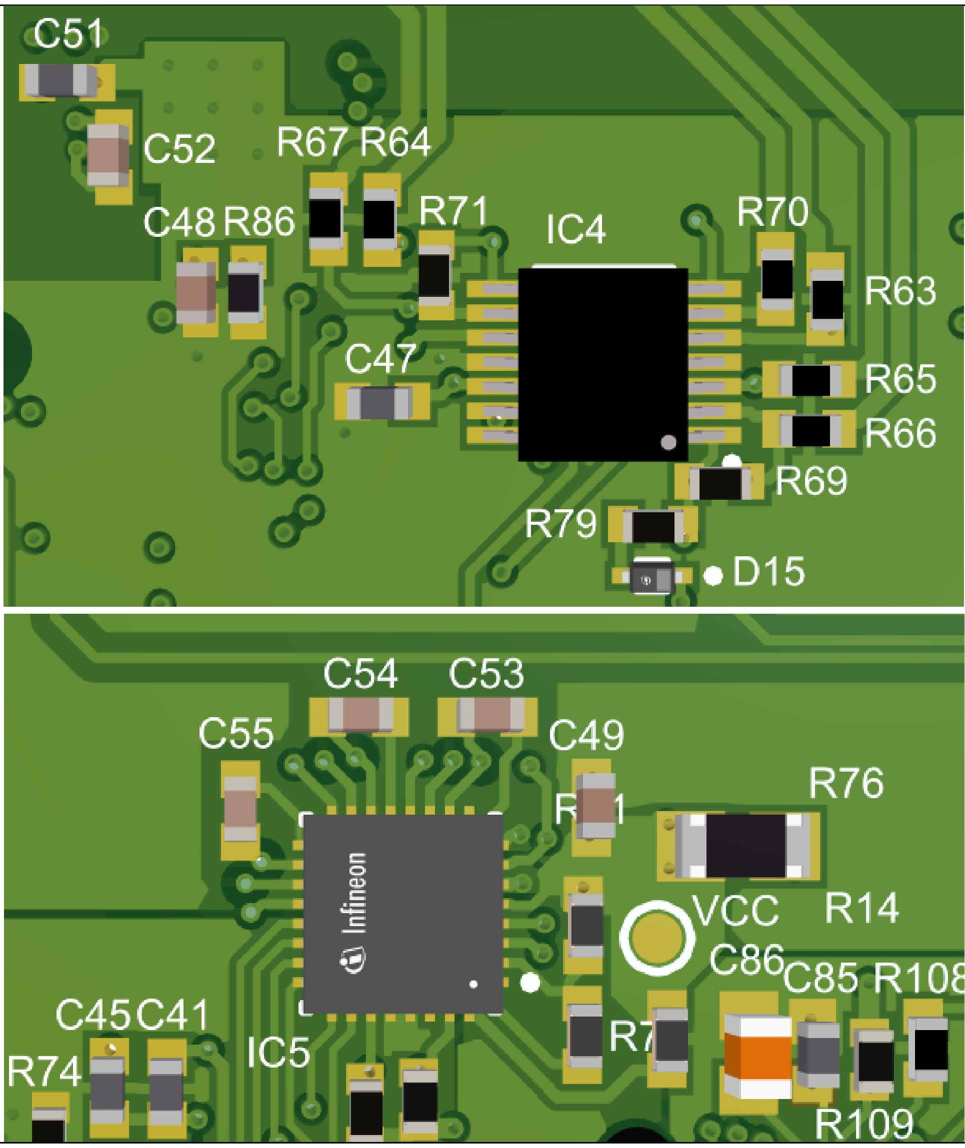

Figure 12 **Current sensing/driving circuitry**

Protection circuitry is integrated into the gate driver design. The gate driver disables the PWM to the power stage when one of the following faults occur:

- Undervoltage lockout
- OCP
- Shoot-through protection
- Deadtime protection

UVLO protection ensures that the IC drives external power devices only when the gate supply voltage is sufficient to fully enhance the power devices. This feature prevents the gates of the MOSFET from being driven with a low voltage that can cause the MOSFET to conduct current while the channel impedance is high, resulting in high conduction losses and possible device failure. Like UVLO, OCP is crucial in any motor drive design. The current level that defines OCP is determined by the shunt resistor connected between the COM and VSS pins (Figure 13). It is also determined by the threshold configured by the ITRIP CONF pin. When overcurrent is detected, the outputs are shut down and RFE is pulled up to VSS.

Shoot-through protection lets through the first input that arrives while the second input causing a shoot-through is held low. As for deadtime protection, a minimum deadtime period is enabled where both the high- and low-side MOSFETs are held off. This lets the first MOSFET be completely switched off before the second MOSFET switches on. The minimum deadtime is automatically inserted whenever the external deadtime is shorter than DT (see the datasheet).

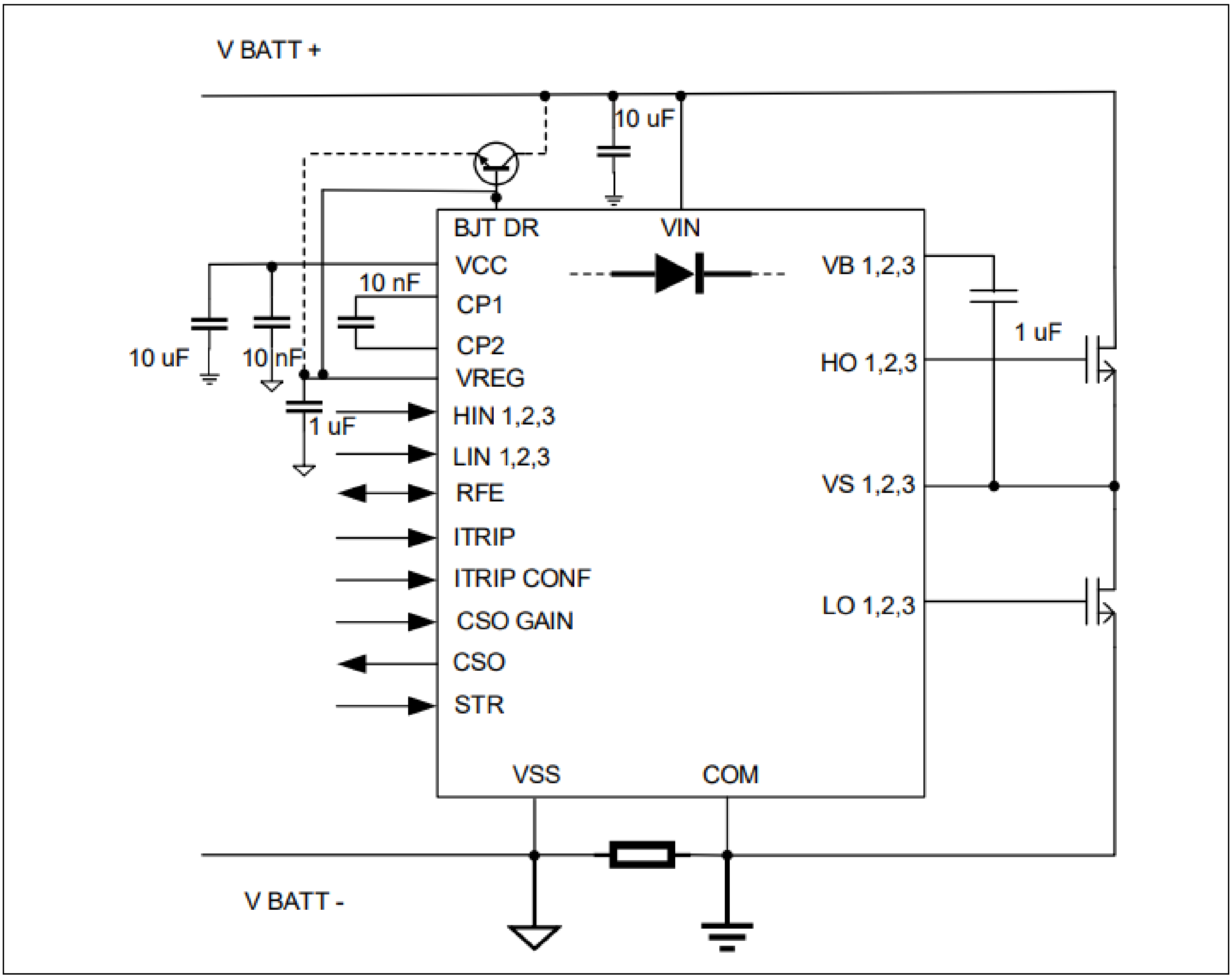

Figure 13 **6ED2742S01Q block diagram**

5 Control and firmware

5.1 Sensorless FOC and trapezoidal control methods

Battery powered OPE is based on BLDC or PMS motors, which are commutated by controlled switching of the inverter instead of using mechanical brushes. Windings are energized in a determined sequence to generate a rotating magnetic field. The rotor's permanent magnet attempts to align with the stator field, producing torque and rotary motion. As with mechanical commutation, electronic commutation helps achieve unidirectional torque similar to a conventional DC machine. In BLDC or PMS motors, the rotor consists of permanent magnets, while the stator is wrapped with a specific number of poles. The rotor position can be sensed using digital Hall effect sensors embedded into the stator. Alternatively, sensorless control algorithms can be used to determine position and speed from the phase currents.

Various control schemes can be used in motor drive applications. The reference board has been designed to support both FOC and trapezoidal control also known as block commutation. FOC is a control method that enables the rotor to follow the stator maintaining a 90° angle between the two flux vectors. The three phase windings are always energized with varying currents in each phase to produce the stator flux angle and magnitude as required. For best performance, three shunts are used to sense the half bridge low side currents, which provide partial phase current feedback sufficient for vector control. Single shunt operation is also possible.

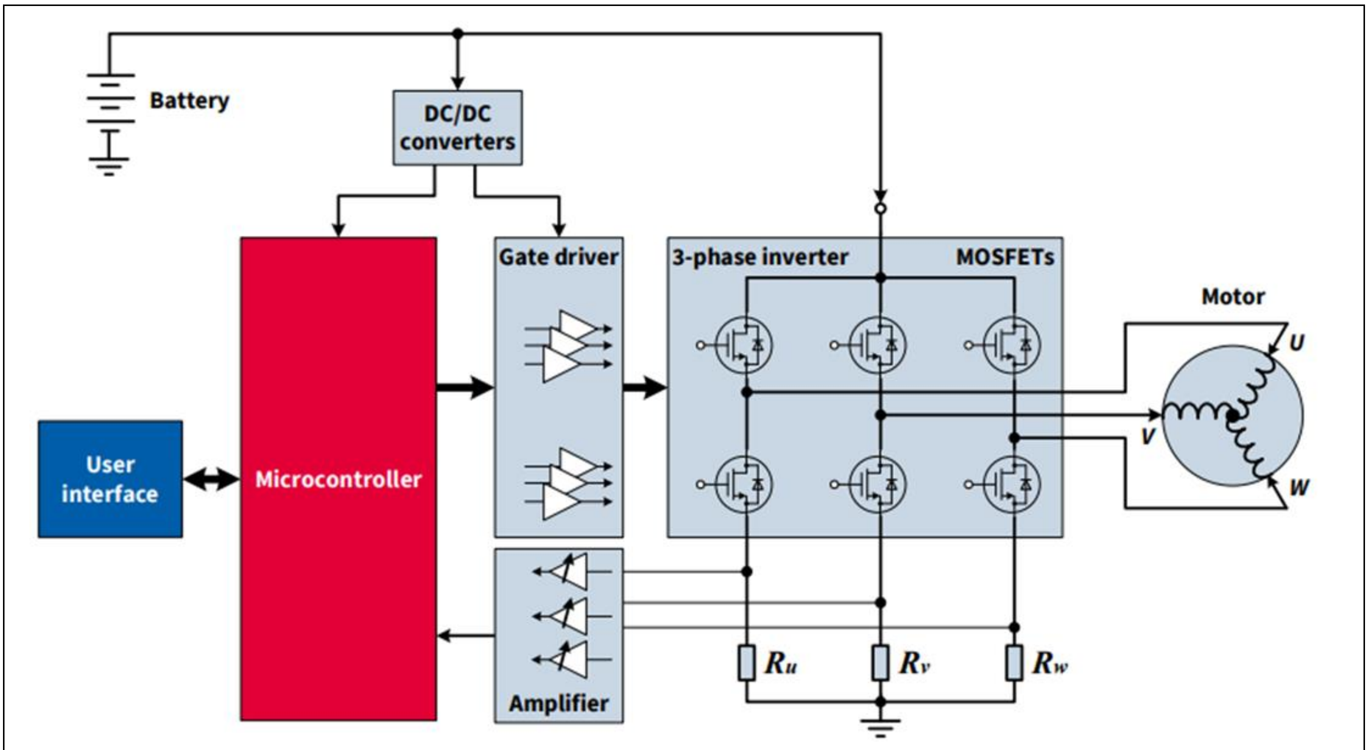

Figure 14 FOC block diagram

These signals are used for sensorless estimation of rotor speed and position. Unlike in block commutation where the angle can vary from 60° to 120°, in FOC, the rotor and stator magnetic flux vectors are kept 90° apart to ensure that maximum torque is applied. By achieving maximum torque, the motor turns optimally and is more efficient due to a low torque ripple, making FOC the preferred control method to use in many applications.

As shown in Figure 15, the three-phase sampled current signals are transformed into two stationary signals using the Clarke transform. The position and rotor speed are then obtained by a sensorless estimator and are used in the Park transform along with the two stationary signals to produce rotating D and Q vectors. Accurate senorless estimation of angle and rotation speed is achieved using calculations in the control firmware and is crucial for keeping the rotor's magnet and the stator field 90° apart.

With FOC, two PI current controllers can be used to control both aspects of the motor current vector separately. One current controller (IQ) is used to control the motor's torque and is thereby called the torque controller; the other one (ID) controls the magnetic flux inside the motor. Transformations are based on the actual rotor angle, acquired by position sensors such as Hall sensors or encoders. The magnetic flux is mainly generated by the rotor so its target value is usually zero, except in special cases like field weakening where a negative value can be applied to achieve higher speed with lower torque. The magnetic flux is targeted to a value of zero so the PI controller can eliminate direct current and reduce energy loss.

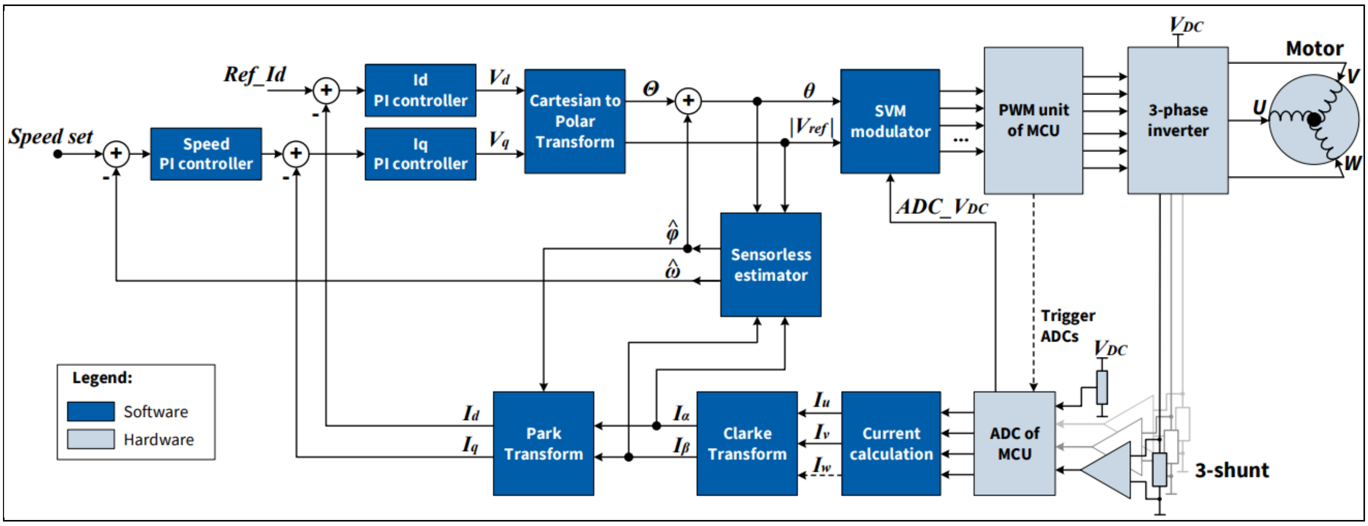

Figure 15 **FOC algorithm block diagram**

On the other hand, block commutation/trapezoidal control is a simpler control method used in BLDC applications. This control method rotates the motor by energizing two phases for 120° during six phases. As shown in Figure 16, all six phases occur during one electrical period and allows only six stator vector positions. Three MOSFETs are active in each position. During turn on, the high-side and low-side MOSFETs are active. The low-side MOSFET stays active during turn on while the high-side turns off and the phase current continues through the body diode of another low-side MOSFET. This causes the angle between the rotor's magnet and stator flux to vary between 60° and 120° as the rotor passes through each sector, which introduces torque ripple. Unlike sensorless FOC, block commutation generally uses Hall or giant magnetoresistance (GMR) sensors to detect the rotor speed and position. The hall sensors then feed back the position to the MCU using hall patterns (Figure 18).

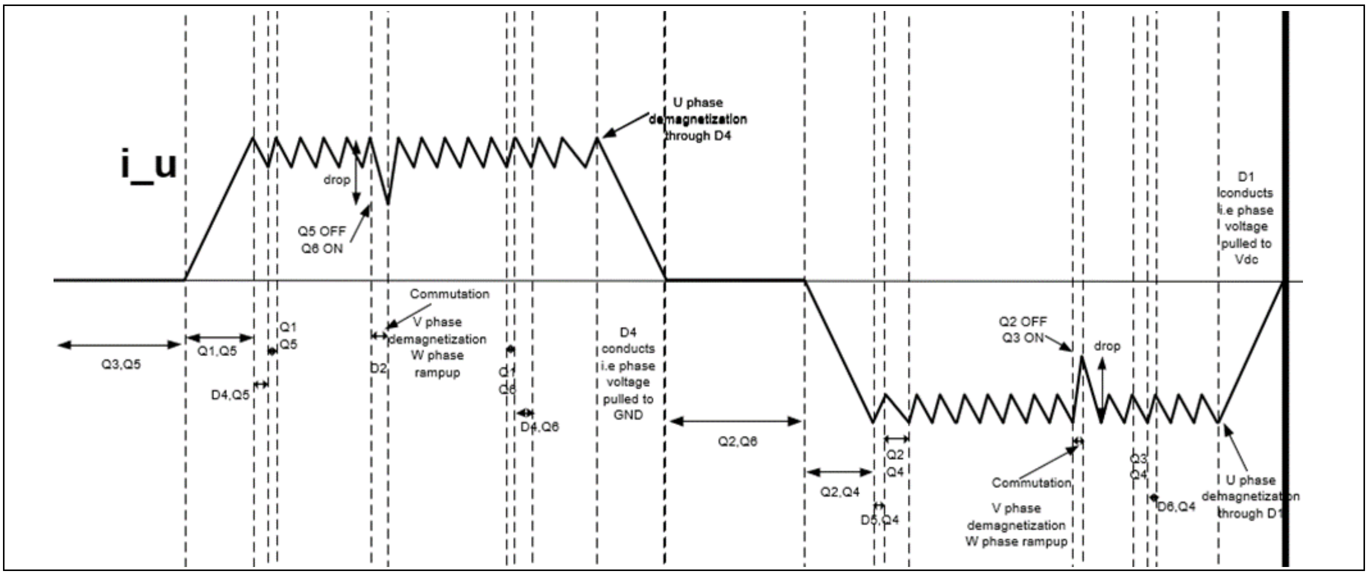

Figure 16 Block commutation electrical period

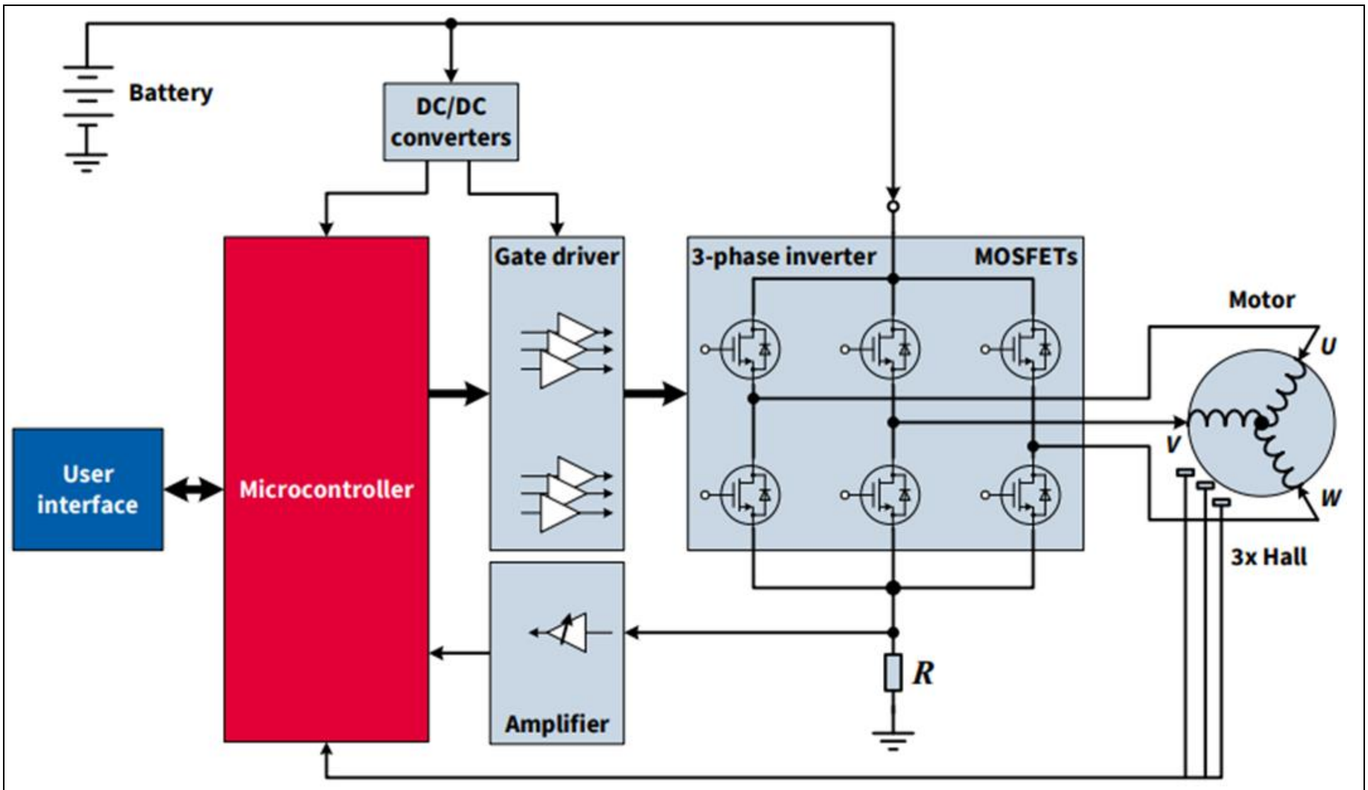

Figure 17 Block commutation block diagram

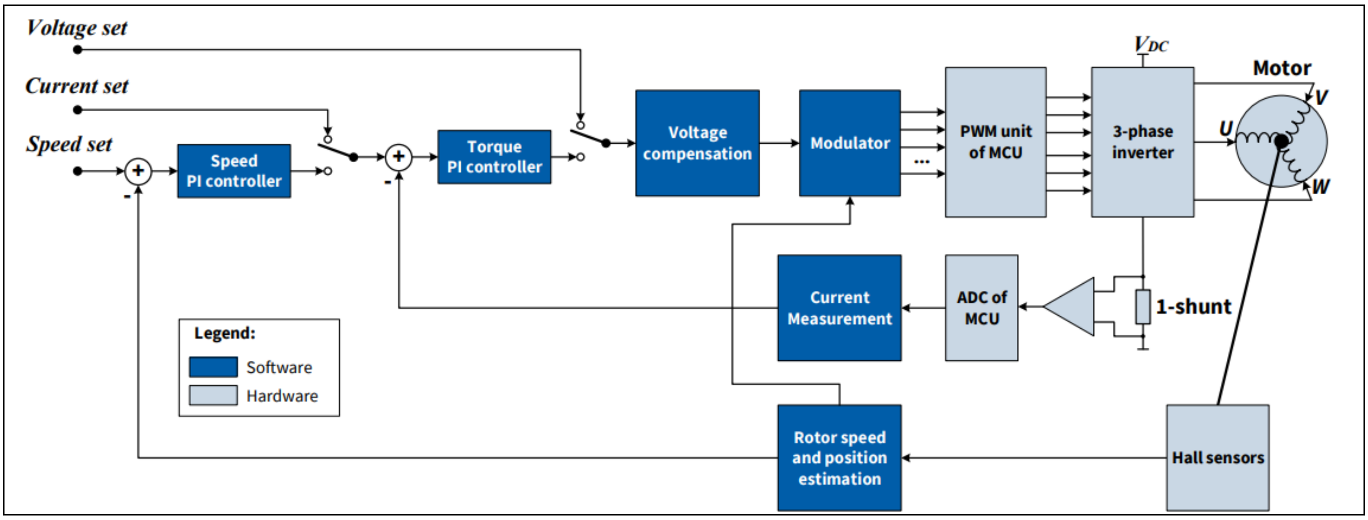

Figure 18 Block commutation algorithm block diagram

FOC and block commutation both differ in hardware and software. As mentioned before, block commutation is a simpler control method. Unlike FOC, block commutation only requires one shunt for current sensing. The Hall sensors are used for sensing the rotor position whereas the position is estimated in FOC by firmware based on the phase currents . The algorithm for FOC is much more complex and requires a complex MCU with greater computing power. The algorithm requires the signals to go through various mathematical transforms and control loops. Though the results are more efficient, great computing power is needed. Hardware comparison between block commutation and FOC is shown here.

Table 1 Hardware comparison of block commutation and FOC

Item	Block commutation	Sensorless FOC	Comments
Three-phase inverter	Six MOSFETs	Six MOSFETs	Normally N-channel MOSFETs
Gate driver	Three half-bridge gate drivers	Three half-bridge gate drivers	
MCU	Low calculation power needed	More calculation power needed	
Typical power supply for the gate driver	+12 V	+12 V	Other possibilities range from +7 V to 15 V
Typical power supply for the MCU	+5 V, from buck converter or LDO	+5 V, from LDO preferably	5V provides more resolution per ADC least significant bit (LSB). Therefore 5 V is preferred in FOC
Current sensing	One leg shunt	Three leg shunts	
Current sensing amplifiers	One amplifier	Three amplifiers	Three amplifiers allow higher performance in slew rate, bandwidth, and offset error
Rotor sensor	Three hall sensors	None	FOC uses software to estimate rotor position

5.2 Implementation of field oriented control

Sensorless (SL) FOC based on Infineon's Motor Control Firmware Solution is implemented on the REF_40VDC_1.5KW_SAW reference board. The overall block diagram of the SL FOC control method is shown below (Figure 19).

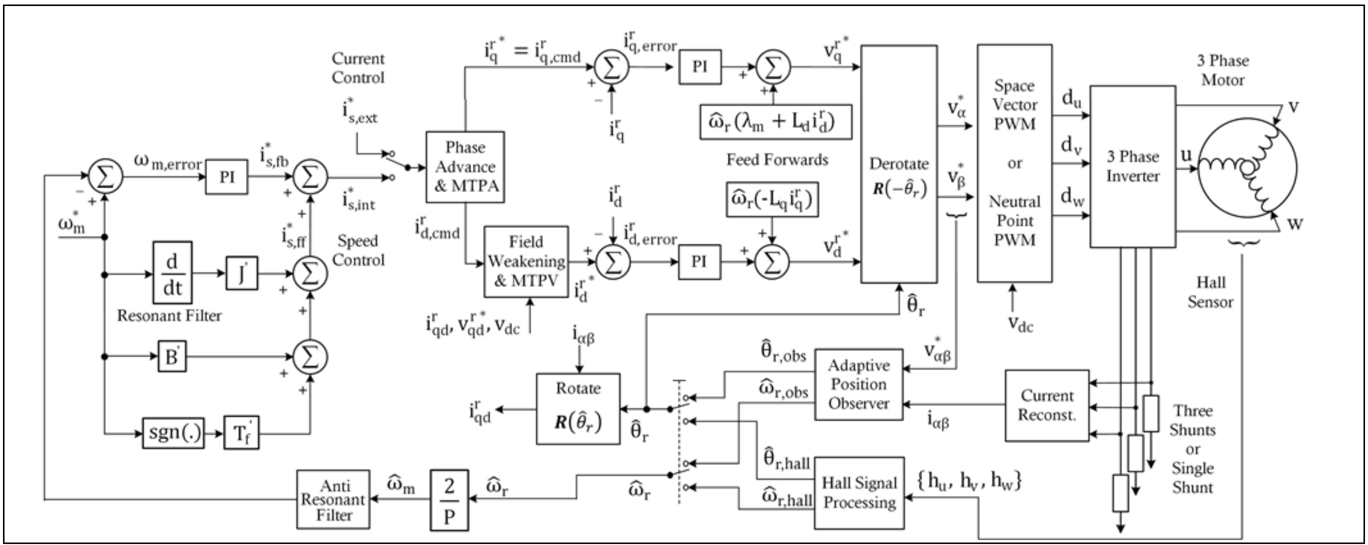

Figure 19 SL FOC block diagram

The rotor's position information is required to extract the speed and control the q and d axis currents. The position and speed information can be obtained by either using a position sensor (such as encoder, resolver, or hall sensors) or through a sensorless approach. The speed controller uses the speed information to create a current reference using a PI controller.

5.3 Speed controller

The parameters of the speed controller are significantly impacted by the mechanical load. Figure 20 shows the mathematical model of the mechanical load driven by the motor and electrical drive system. This model includes T_f (coulombic friction), B (viscous friction), and J (inertia).

When using the firmware to operate any motor, it is crucial to accurately measure or estimate these three parameters and input them into the GUI or hardcode them in the appropriate header files. The speed controller's kp and ki, and the feedforward terms are directly derived from these parameters, as explained further later.

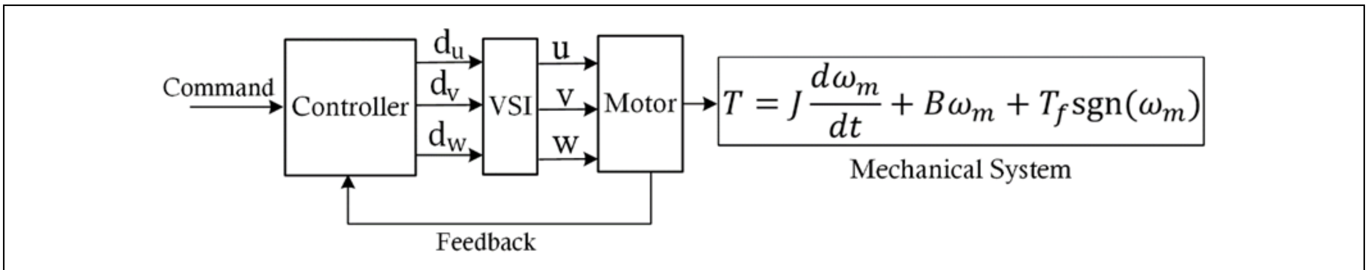

Figure 20 Mechanical load run by the motor and drive system

To derive the value of proportional, integral, and the feedforward terms of the speed controller, the speed loop block diagram along with a simple model of motor and mechanical load is used, as shown in Figure 20, where:

$$k_t \approx \left(\frac{3}{2}\right)\left(\frac{P}{2}\right)\lambda_m \tag{1}$$

Pole-zero cancellation technique is used to find the PI controller integral and proportional gain. By having

$$\frac{k_i}{k_p} = \frac{B}{J} \tag{2}$$

the controller zero cancels the mechanical load's pole. The PI controller coefficients are also proportional to speed loop bandwidth, as shown here:

$$k_i \propto B\omega_{BW} \tag{3}$$
$$k_p \propto J\omega_{BW} \tag{4}$$

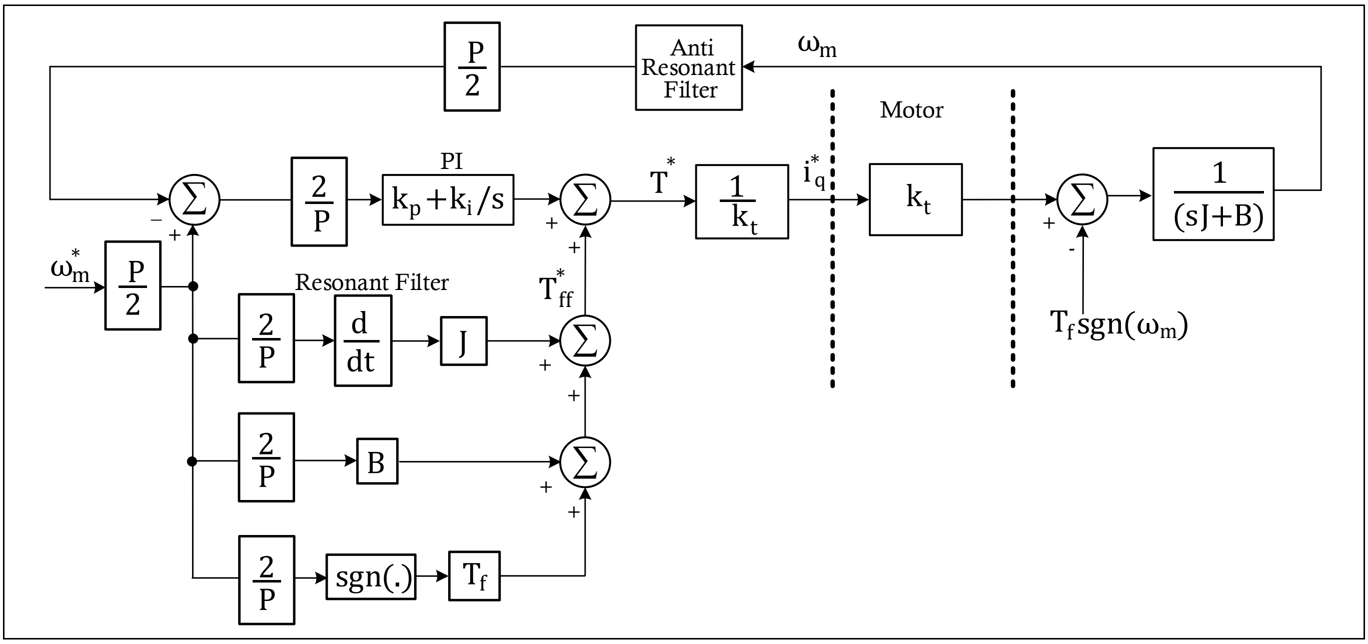

Figure 21 RFO speed control block diagram before rescaling the parameter

The proportional and integral gains are ultimately determined after being rescaled to account for the motor parameters k_t and P. Figure 20 demonstrates how k_t and P, as shown in Figure 21, can be integrated into the controller parameters, leading to the new updated forms:

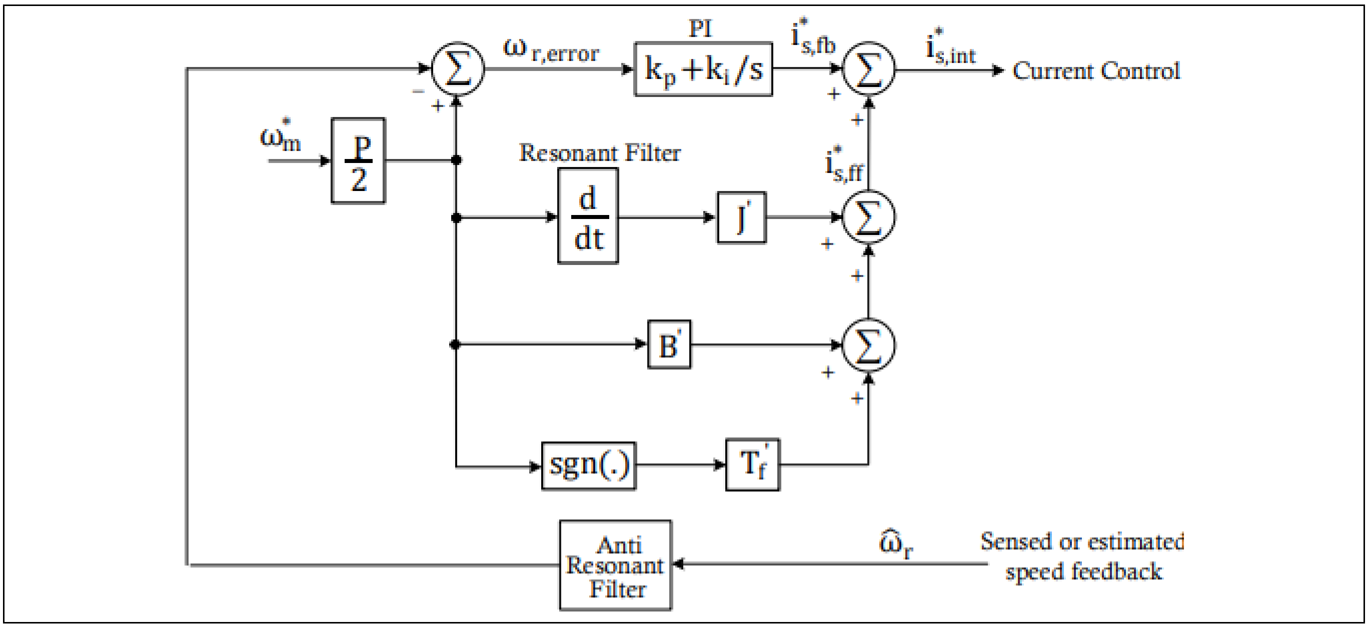

Figure 22 RFO speed loop block diagram before rescaling the parameters

After rescaling, the speed controller parameters are:

$$k_i = \left(\frac{1}{k_t}\right)\left(\frac{2}{P}\right)B\omega_{BW} = \left(\frac{8}{3}\right)\left(\frac{1}{P^2}\right)\left(\frac{1}{\lambda_m}\right)B\omega_{BW} \quad (5)$$

$$k_p = \left(\frac{1}{k_t}\right)\left(\frac{2}{P}\right)J\omega_{BW} = \left(\frac{8}{3}\right)\left(\frac{1}{P^2}\right)\left(\frac{1}{\lambda_m}\right)J\omega_{BW} \quad (6)$$

The feedforward terms can also be updated as:

$$B' = \left(\frac{1}{k_t}\right)\left(\frac{2}{P}\right)B = \left(\frac{8}{3}\right)\left(\frac{1}{P^2}\right)\left(\frac{1}{\lambda_m}\right)B \quad (7)$$

$$J' = \left(\frac{1}{k_t}\right)\left(\frac{2}{P}\right)J = \left(\frac{8}{3}\right)\left(\frac{1}{P^2}\right)\left(\frac{1}{\lambda_m}\right)J \quad (8)$$

$$T_f' = \left(\frac{1}{k_t}\right)T_f = \left(\frac{4}{3}\right)\left(\frac{1}{P}\right)\left(\frac{1}{\lambda_m}\right)T_f \quad (9)$$

The feedforward terms in the speed loop are affected by both mechanical load and motor parameters. These three feedforward terms play a role in enhancing the dynamic performance of the speed loop. The inertia term utilizes a second-order resonant filter to estimate the acceleration, aiming to mitigate the potential impact of the noise that could arise if a direct derivation method had been employed.

5.4 Phase Advance and MTPA

The MTPA block is responsible for generating command values for q and d axis currents ($\mathrm{i}_\mathrm{q}^\mathrm{r}$ and $\mathrm{i}_\mathrm{d}^\mathrm{r}$) to maximize the torque for the overall current injected in the motor winding. The torque equation of the PMSM motor is written in (1) as:

$$\mathrm{T} = \frac{3P}{4}\left(\lambda_m \mathrm{i}_\mathrm{q}^\mathrm{r} + \left(L_d - L_q\right)\mathrm{i}_\mathrm{q}^\mathrm{r}\mathrm{i}_\mathrm{d}^\mathrm{r}\right) \tag{1}$$

The d and q axis current commands $\mathrm{i}_\mathrm{d,cmd}^\mathrm{r}$ and $\mathrm{i}_\mathrm{q,cmd}^\mathrm{r}$ need to be obtained from the reference current magnitude i_s^* generated by the output of the speed controller as follows:

$$\begin{aligned} i_{d,\mathrm{cmd}}^{r} &= i_s^* \sin\theta \\ i_{q,\mathrm{cmd}}^{r} &= i_s^* \cos\theta \end{aligned} \tag{2}$$

where θ is the angle of the current i_s^* with respect to rotor q axis.

Plugging (2) into (1) and rearranging the whole equation yields the torque equation as a function of θ as:

$$\mathrm{T} = \frac{3P}{4}\left(\lambda_m i_s^* \cos\theta + \frac{\left(L_d - L_q\right)}{2} {i_s^*}^2 \sin 2\theta\right) \tag{3}$$

To find the maximum of the torque function, the equation below needs to be solved:

$$\frac{dT}{d\theta} = 0 \tag{4}$$

which results in,

$$\sin\theta = \frac{\sqrt{{\lambda_m}^2 + 8\left(L_d - L_q\right)^2 {i_s^*}^2} - \lambda_m}{4\left(L_d - L_q\right) i_s^*} \tag{5}$$

Plugging (5) back into (2) and rearranging, results in MTPA current command values are as follows:

$$\begin{aligned} \mathrm{i}_\mathrm{d,MTPA}^\mathrm{r} &= \frac{\lambda_m - \sqrt{{\lambda_m}^2 + 8\left(L_q - L_d\right)^2 {i_s^*}^2}}{4\left(L_q - L_d\right)} \\ \mathrm{i}_\mathrm{q,MTPA}^\mathrm{r} &= \sqrt{{i_s^*}^2 - {\mathrm{i}_\mathrm{d,MTPA}^\mathrm{r}}^2} \cdot \mathrm{sgn}(i_s^*) \end{aligned} \tag{6}$$

5.5 Flux Weakening and MTPV

Flux weakening (field weakening) is a method to increase the speed of the motor beyond its base speed. At base speed, the inverter voltage becomes saturated which means that there would not be enough voltage generated on the inverter to overcome the back EMF of the motor and increase the speed above the base speed. Therefore, the flux wakening method is needed to reduce the back EMF voltage of the motor and further increase the speed. Figure 23 shows the flux weakening controller for RFO.

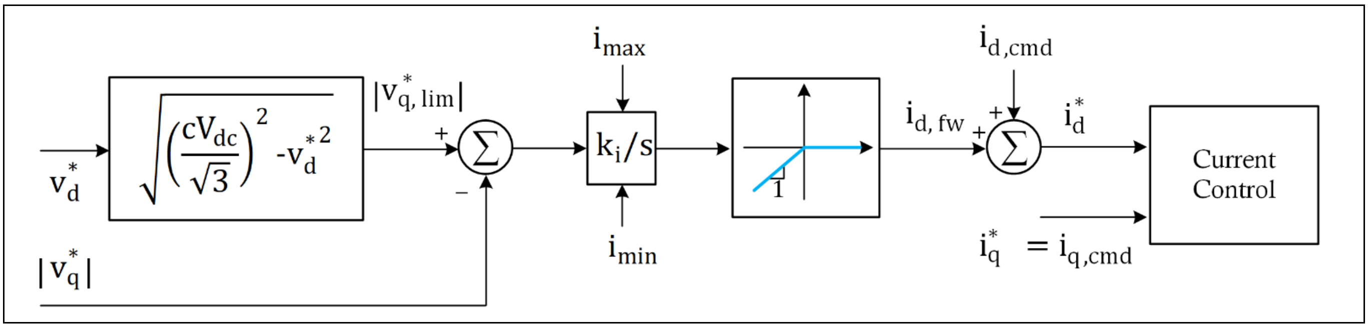

Figure 23 Flux weakening method

As mentioned, the controller requires more voltage (V_q^*) than the inverter $V_{q,\text{lim}}^*$ can produce above the base limit. Note that the coefficient $c = 0.90{\sim}0.95$ used for the voltage limit is needed to leave some margin before the absolute voltage limitation is reached, to avoid instability. The voltage error required to increase the motor speed is passed through an integrator to generate the amount of the current in d axis for weakening the flux and enable speed increase. Note that the current generated by the integrator needs to be limited as follows:

$$i_{\text{max}} = \min\left(KI_{d,\text{max}}, \sqrt{I_{\text{lim}}^2 - i_{q,\text{fb}}^2}\right) - i_{d,\text{cmd}} \quad (7)$$
$$i_{\text{min}} = \max\left(-I_{d,\text{max}}, -\sqrt{I_{\text{lim}}^2 - i_{q,\text{fb}}^2}\right) - i_{d,\text{cmd}}$$

Where,
$\text{K} = 0.05$ is a coefficient to increase the d axis current saturation level more than zero
$\text{I}_{\text{d,max}}$ is the maximum d axis current allowed in the motor
I_{lim} is the maximum three-phase current allowed in the motor windings, which is determined by the I^2T protection algorithm
The field weakening current must always be a negative current and be added to the MTPA current command $i^r_{d,cmd}$.

In (7), $I_{d,\text{max}}$ needs to be selected based on the maximum allowed current of the motor, and at the same time, it must not exceed the level where demagnetization would occur in the rotor magnets. I_{lim} is also the output of I^2T.

5.6 Current controller

The d and q current commands are used as an input for the current controllers and the output will be the voltage references. The voltage references v_d^{r*} and v_q^{r*} are eventually applied to the motor using the inverter to control the current. This means that the voltages are considered as an input to the model of the PMSM machine as,

$$v_d^{r*} = R_s i_d^r + L_d \frac{di_d^r}{dt} - \omega_r\left(L_q i_q^r\right) \quad (8)$$
$$v_q^{r*} = R_s i_q^r + L_q \frac{di_q^r}{dt} + \omega_r(\lambda_m + L_d i_d^r)$$

In these equations, the d and q axis currents are not decoupled, and one has a dependency to the other. To decouple this dependency and simplify the equations for the control system, feedforward terms can be added to the output of the current controllers according to Figure 19 and reduce the PMSM system to,

$$v_d^{r*} = R_s i_d^r + L_d \frac{di_d^r}{dt}$$
$$v_q^{r*} = R_s i_q^r + L_q \frac{di_q^r}{dt} \quad (9)$$

Now a PI controller can be easily designed for these set of equations with the equivalent control block diagram shown here:

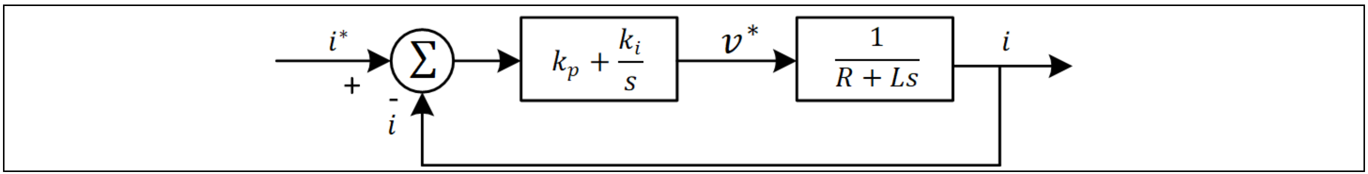

Figure 24 Current controller block diagram

In the closed loop system in Figure 24, it is preferred to cancel the pole of the system with the zero of the PI controller to reduce the order of closed loop system and controller design simplification. Hence,

$$\frac{k_p}{k_i} = \frac{L}{R} \quad (10)$$

This will reduce the closed loop transfer function of the system to,

$$H_{cl} = \frac{k_i}{Rs} = \frac{k_p}{Ls} \quad (11)$$

which can be used to calculate the PI controller coefficients for a given system bandwidth ω_c as,

$$k_p = \omega_c L$$
$$k_i = \omega_c R \quad (12)$$

6 Test setup

Various tests were performed on the reference board using the test setup shown in the block diagram below. The oscilloscope along with the voltage and current probes were used to obtain waveforms at various speed and load conditions. The power analyzer was used to measure the efficiency of the reference board at different loads. The board can be controlled using its on-board speed and direction controls or through the ModusToolbox™ Motor Suite software tool (V 2.4.0 or higher), which you can download through the Infineon Developer installer.

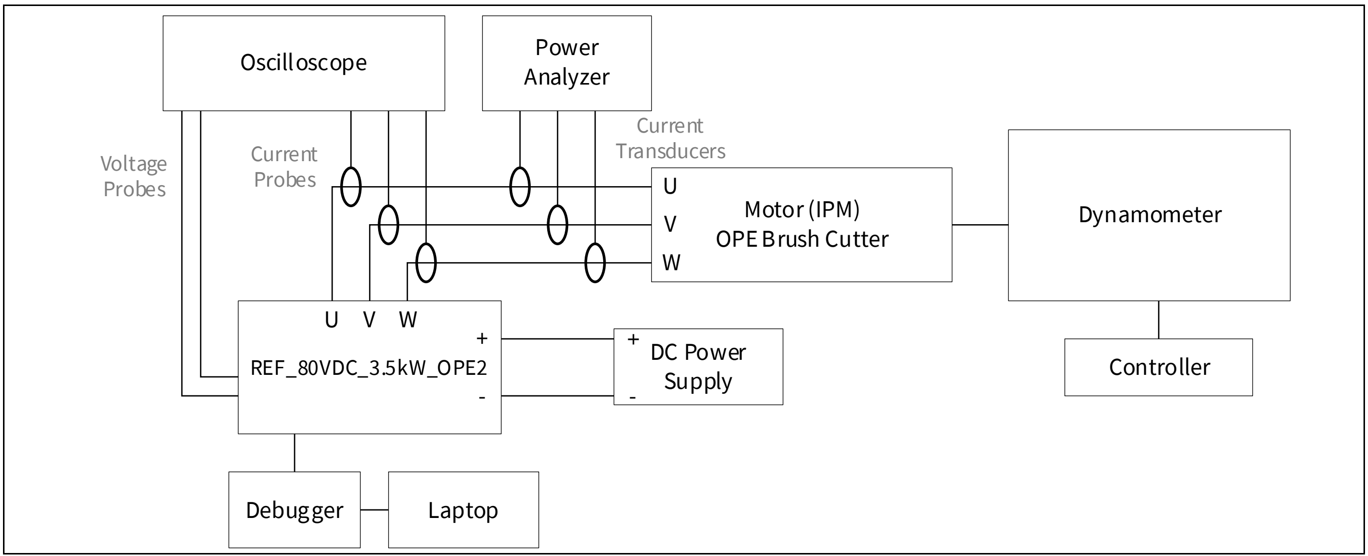

Figure 25 Test setup

The test results were obtained using a Magtrol dynamometer. The dynamometer acts as an adjustable mechanical load connected to the test motor and used to measure torque and speed. The reference board was tested under various loads and different speeds, making the dynamometer a practical piece of equipment to use. A blower is connected to the dynamometer and is turned on during testing to prevent the piece of equipment from overheating. In addition, a high-speed programmable controller is connected to the dynamometer and is used to control the torque.

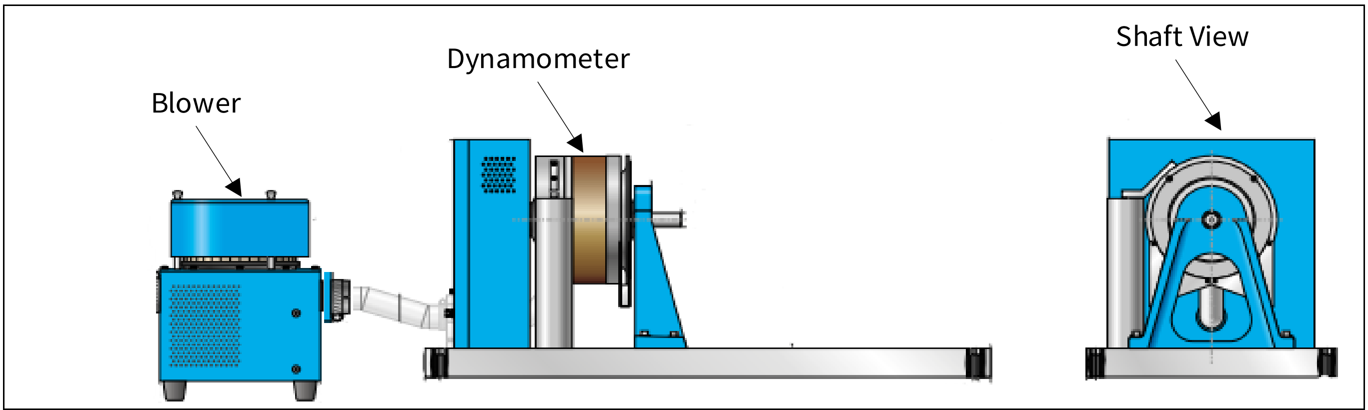

Figure 26 Magtrol dynamometer setup

7 Operating the board using the motor control GUI

The reference board must be set up in order to drive a motor. Figure 27 shows the external connections used to connect the motor phases, debugger, power supply, and Hall sensor inputs. Figure 27 also shows the control switches you can use if you are not using the GUI. It is important to ensure the potentiometer is positioned to zero (rotated fully counter-clockwise) before powering up the board. Once you have made the external connections, you can set the power supply using the proper voltage and current limits and enable it (see specifications).

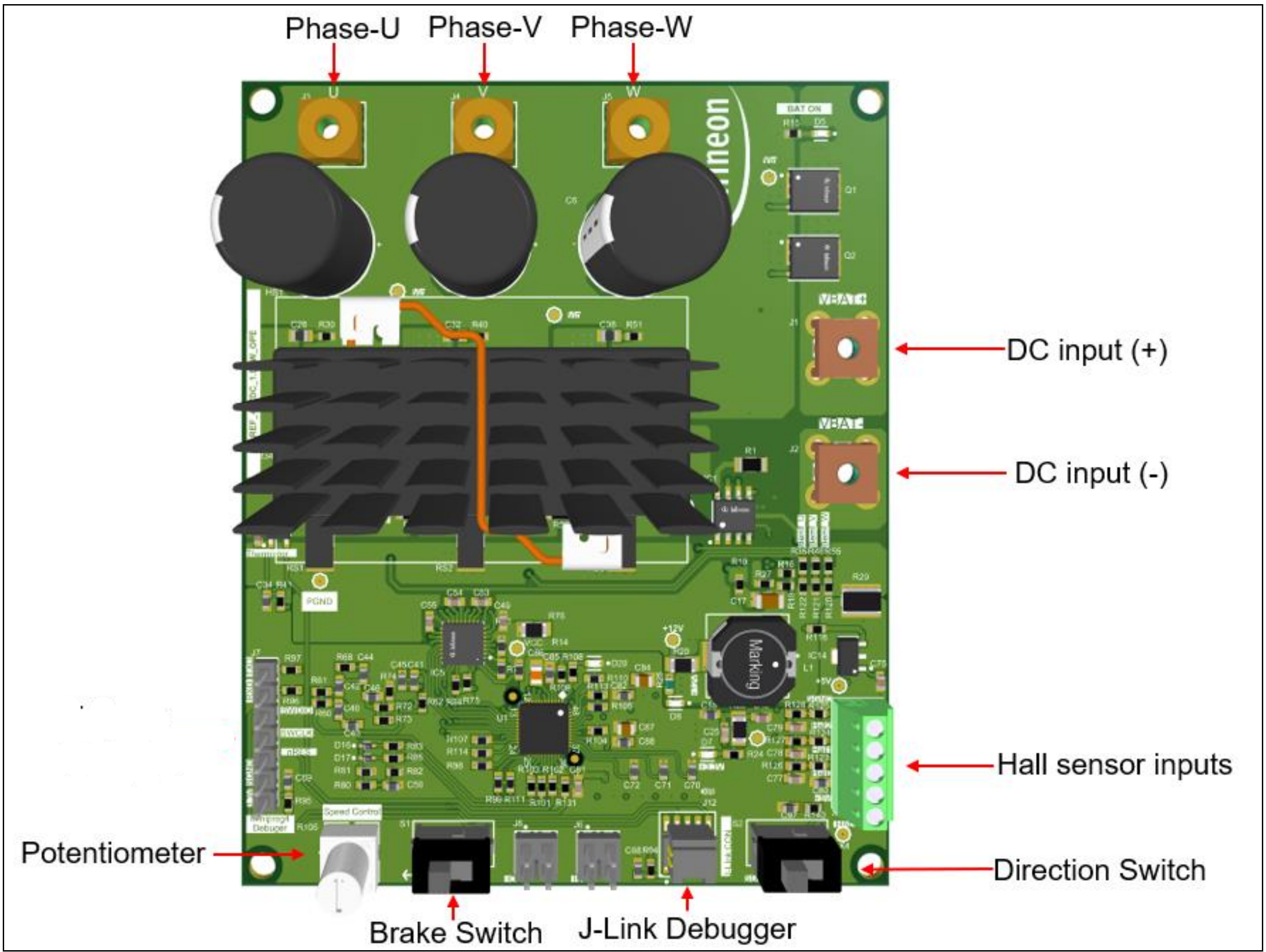

Figure 27 REF_40VDC_1.5KW_SAW external connections and controls

1. Connect the motor cables to the phase terminals on the board (cable order does not matter)
2. Connect the power supply to VBAT+ and VBAT- terminals
3. Set the power supply to 24 V and the current limit to 0.5 A but do not enable the power supply
4. Set the potentiometer to zero (rotate the knob counter-clockwise until it cannot turn anymore)
5. Connect the J-link debugger to the power board.
6. Enable power supply. Ensure that D5, D7, and D8 are lit up

The motor control GUI downloads control firmware and configuration settings for the MCU on the motor control boards operating with FOC with one or three shunts. You can use the workbench to select the parameters for a project and then save the configuration. The steps to downloading the GUI are:

1. Download the Infineon Developer Center Launcher application and log in using your Infineon credentials
2. Once the **Developer Center Launcher** is downloaded, go to **Manage tools** and search for **ModusToolbox™ Motor Suite (V 2.4.0)** on the search bar to install it
3. Click **Start** on ModusToolbox™ Motor Suite
4. Select **PSOC™ Control C3** and **RFO** on the dropdown menu to create a new project, as show on Figure 28
5. Connect the other end on the J-link Debugger to the computer (USB port).
6. Enable power supply and connect the GUI to the board through the GUI, as shown on Figure 29

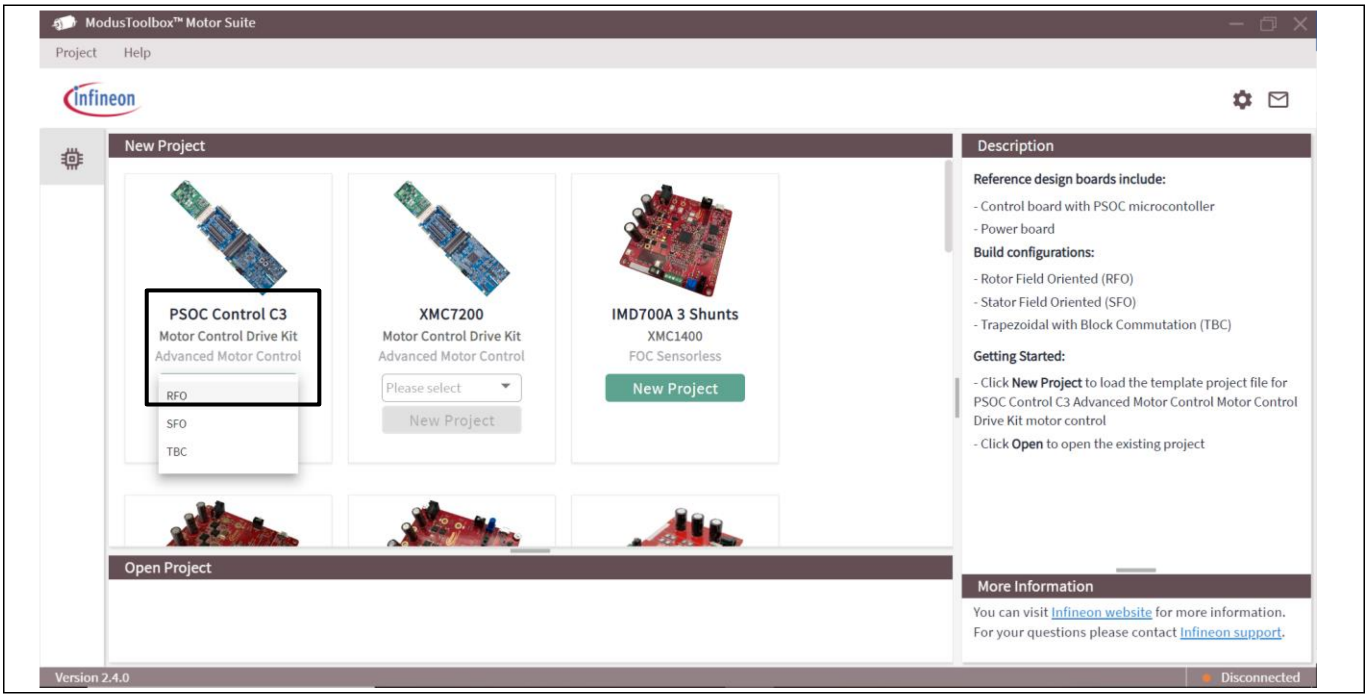

Figure 28 Motor control GUI launch screen

7. On the bottom-right of the configuration page, select **Disconnected** > **Segger Serial No** to enable the power supply and connect the GUI to the board

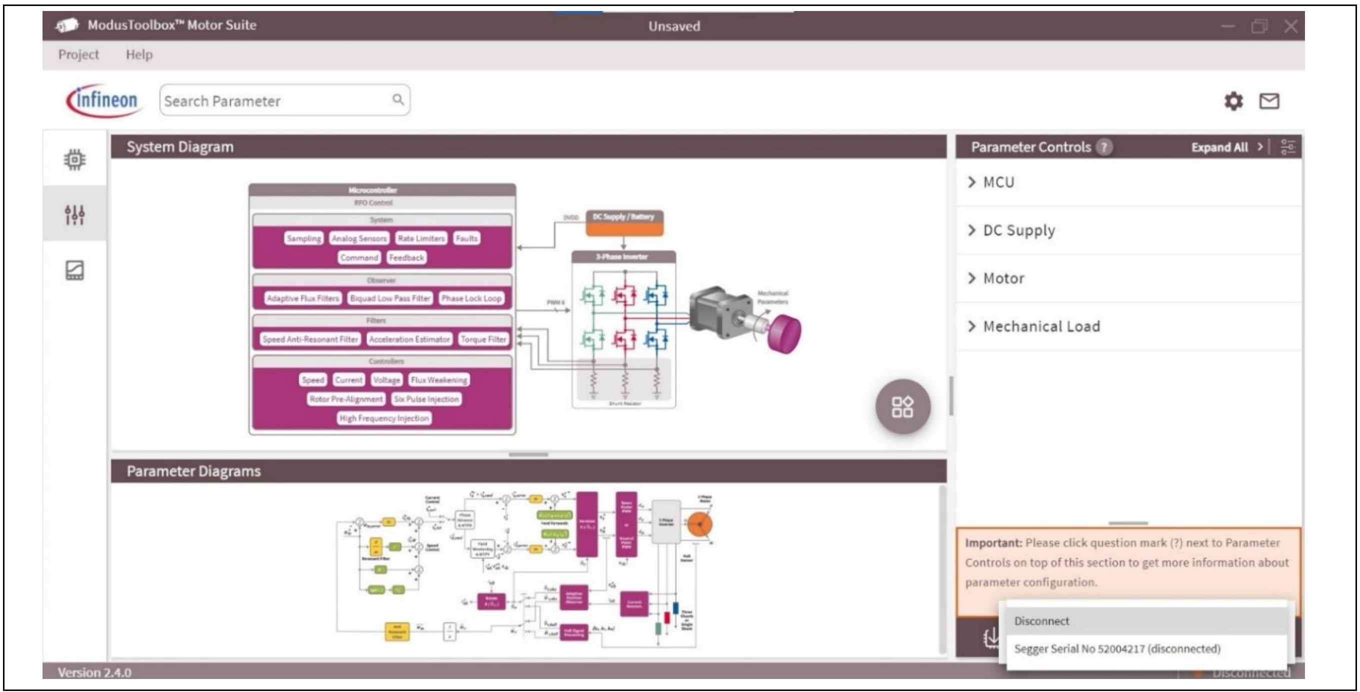

Figure 29 Connecting the GUI to the board

8. Select the **Flash Firmware** icon on the bottom right-hand side of the screen. A separate window should appear.
9. Select **Browse** and then select **Yes** to continue as shown in Figure 30
10. Select the hex file and then **Flash** as shown in Figure 31. The GUI should take about half a minute to process the hex file. Once it is done, another window will pop up. If the GUI is unable to read the hex file try to close the GUI completely and start from step 3.

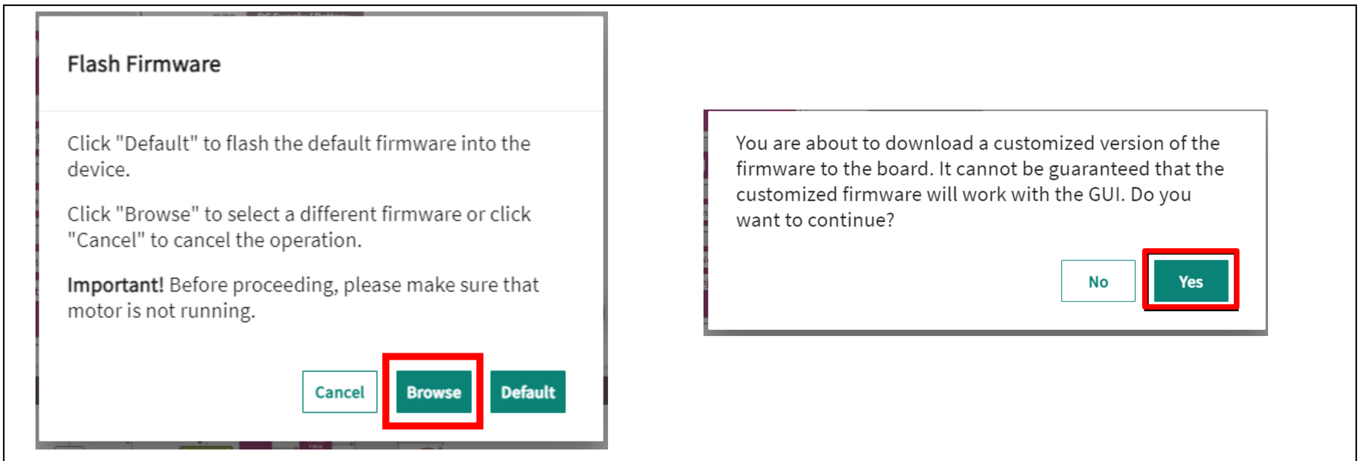

Figure 30 Flashing firmware

11. Click **Select File** and upload the elf file. A window on the bottom right hand corner will appear once the elf file has been read.

Operating the board using the motor control GUI

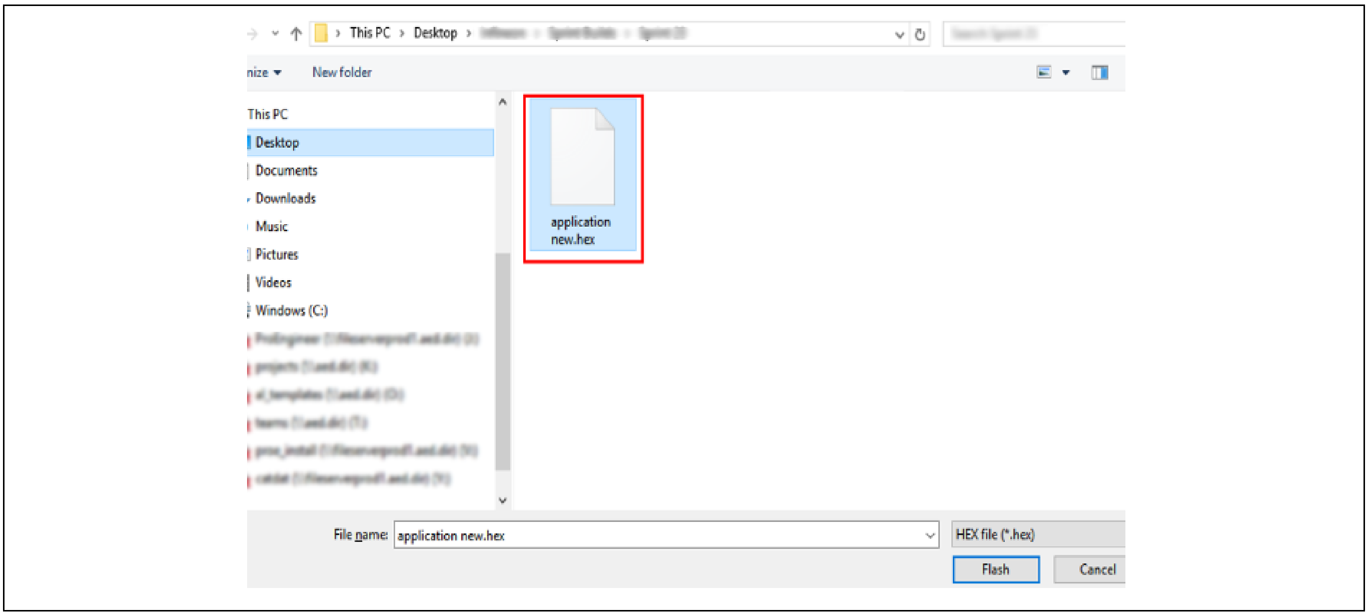

Figure 31 Flashing the parameters

12. Go to the test bench by selecting the oscilloscope icon on the left of the screen as shown on Figure 32
13. On the **Command panel**, enable **Drive** and start running the board by turning off **Potentiometer Control** and sliding the **Target Set** to your desired speed. If you prefer to run the board using the potentiometer on the board, turn on the **Potentiometer Control** on the **Command panel** and increase the speed using the potentiometer on the board

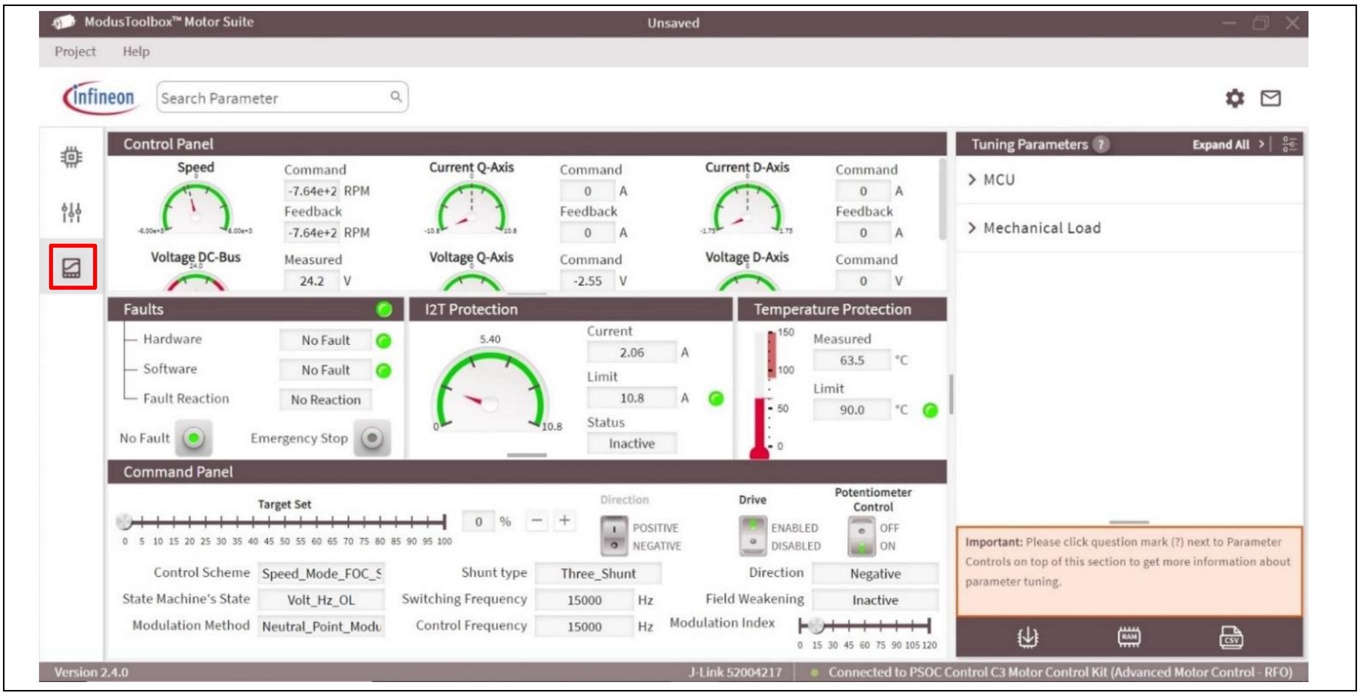

Figure 32 GUI test bench

8 Bill of materials

Reference	Qty	Type	Value/rating	Manufacturer	Part number
C1	1	Capacitor	10uF, 100V, 20%, 1210, X7S	MuRata	GRM32EC72A106ME05L
C2, C18, C21, C34, C46, C47, C51, C68, C69, C74, C76, C80, C82, C85, C88, C90, C92, C100, C102, C104	20	Capacitor	100nF, 50V, 10%, 0603	Kemet	C0603C104K5RACAUTO
C3	1	Capacitor	22nF, 50V, 10% , 0603, X8R	TDK Corporation	C1608X8R1H223K080AE
C4	1	Capacitor	2.2nF, 100V, 20%, 0603, X7R	TDK Corporation	CGA3E2X7R1H222K080A A
C5	1	Capacitor	2.2nF, 250V, 10%, 0805, X7R	Yageo	CC0805KRX7RYBB222
C6, C7, C8	3	Polarized	560UF, 63V, 20% , RADIAL TH	Chemi-Con	661-EKZE630ELL561MK3
C9, C10, C11, C12, C13, C14, C26, C27, C30, C31, C36, C37	12	Capacitor	1uF, 100V, 10%, 0805, X7S	Murata	GRJ21BC72A105KE11L
C15	1	Capacitor	2.2nF, 50V, 5%, 0805, C0G	TDK Corporation	CGA4C2C0G1H222J060AA
C16	1	Capacitor	2.2nF, 50V, 20%, 0603, X7R	TDK Corporation	CGA3E2X7R1H222K080A A
C17	1	Capacitor	2.2uF, 100V, 10% , 1206, X7R	Samsung	CL31B225KCHSNNE
C19, C49	2	Capacitor	10uF ,25V, 20% , 0603, X5R	Wurth Elektronik	885012106031
C20, C33, C73, C75, C99, C107	6	Capacitor	1uF, 25V, 10%, 0603, X7R	Wurth Elektronik	885012206076
C22	1	Capacitor	47pF, 50V, 5%, 0603, C0G	TDK Corporation	CGA3E2NP01H470J080AA
C23, C24	2	Capacitor	10uF, 25V, 10% , 1210, X7R	Samsung	CL32B106KAJNNNE
C25	1	Capacitor	10nF, 25V, 10%, 0603, X7R	Wurth Elektronik	8.85012E+11
C28, C29, C32, C35, C38, C39	6	Capacitor	10000PF ,100V, 10%, 0805	Samsung	CL21B103KCANNNC

Reference	Qty	Type	Value/rating	Manufacturer	Part number
C40, C41, C42, C43, C44, C45, C50, C97, C108	9	Capacitor	100pF, 50V, 1%, 0603, C0G	Kemet	C0603C101F5GACAUTO
C48	1	Capacitor	1nF, 25V, 10%, 0603, X7R	MuRata	GCJ188R71E102KA01D
C52, C81, C93, C101	4	Capacitor	10nF, 50V, 10%, 0603, X7R	MuRata	GCM188R71H103KA37J
C53, C54, C55	3	Capacitor	1uF, 25V, 10%, 0603, X7R	MuRata	GCJ188R71E105KA01J
C70, C71, C72	3	Capacitor	1nF, 50V, 10%, 0603, X7R	Kemet	C0603C102K5RECAUTO
C77, C78, C79	3	Capacitor	330pF, 100V, 2%, 0603, C0G	MuRata	GCM1885C2A331JA16D
C83, C84, C87, C89, C91	5	Capacitor	10uF, 10V, 10%, 0805, X7R	MuRata	GRM21BR71A106KA73K
C86	1	Capacitor	4.7uF, 50V, 10%, 0805, X7R	TDK Corporation	CGA4J1X7R1H475K125AE
C94, C95, C96	3	Capacitor	330pF, 50V, 10%, 0603, X7R	Wurth Elektronik	8.85012E+11
C98	1	Capacitor	1uF, 16V, 10%, 0603, X5R	MuRata	GRM185R61C105KE44J
D2, D3, D4, D9, D10, D11, D12, D13, D14, D15, D16, D17	12	Diode	30V, 500MA, SC79-2	Infineon Technologies	BAS3005A02VH6327XTSA1
D5, D7, D8	3	LED	LED GREEN DIFFUSED 0603 SMD	ams-OSRAM USA INC.	LG Q396-PS-35-0-20-R18
D6	1	Diode	200V, 3A, DO214AA	ON Semiconductor	S320
D19, D22, D23, D24, D25, D26, D27	7	Diode	30V, 200MA, SOT23	Vishay	BAT54S-E3-08
D20	1	LED	LED YELLOW DIFFUSED 0603 SMD	ams-OSRAM USA INC.	LY Q396-P1Q2-36-0-10-R18
D21	1	LED	LED RED CLEAR 0603 SMD	Dialight	5988010107F

Reference	Qty	Type	Value/rating	Manufacturer	Part number
HS1	1	Heatsink	Heat Sink, 31.90 mm L X 50.00 mm W X 35.00 mm H body	Alpha and Omega Semiconductors	S001ZBGX
IC1	1	IC	Neptune, M1957, A12	Infineon Technologies	1EDL8011
IC2	1	IC	REG, BUCK, ADJ, 1A, 8SOPWR	Texas Instruments	LM5164QDDATQ1
IC3	1	IC	Linear, PG-DSO-8-52	Infineon Technologies	TLS203B0EJ V33
IC4	1	IC	CMOS, 4 CIRCUIT, 14TSSOP	Analog Devices	AD8618ARUZ
IC5	1	IC	IC GATE DRVR HALF-BRIDGE 32VQFN	Infineon Technologies	6ED2742S01Q
IC14	1	IC	REG, LINEAR, 5V, 100MA, SOT89-3	STMicroelectroni cs	LD2981CU50TR
J1, J2	2	Connector	TERM REDCUBE M3 4PIN PCB	Würth Elektronik	74650073R
J3, J4, J5	3	Connector	TERM REDCUBE M3 6PIN PCB	Würth Elektronik	7461057
J6, J8	2	Connector	CONN HEADER, VERT, 4POS, 2.54MM	Samtec	TSW-102-07-L-D
J7	1	Connector	CONN HEADER, VERT, 7POS, 2.54MM	Samtec	TSW-107-07-L-S
J12	1	Connector	CONN HEADER, SMD, 10POS, 1.27MM	Samtec	FTSH-105-01-F-DV-007-K-P
L1	1	Inductor	FIXED IND, 68UH, 1.9A ,132 MOHM, SMD	Wurth Elektronik	7447714680
Q1, Q2	2	MOSFET	N-CH ,60V, 32A , PG-TDSON-8 FL	Infineon Technologies	ISC015N06NM5LF2ATMA 1

Reference	Qty	Type	Value/rating	Manufacturer	Part number
Q3, Q4, Q5, Q6, Q7, Q8	6	MOSFET	N-CH, Enhancement , 60V, 510A , PG-TSON-12-1	Infineon Technologies	IQFH61N06NM5
R1	1	Resistor	0R , 0.25W, 1% , 1206	Yageo	RC1206JR-070RL
R2, R6, R25	3	Resistor	10k, 0.1W, 0.1%, 0603	Vishay	TNPW060310K0BYEA
R3	1	Resistor	1R, 0.5W, 1%, 0805	Vishay	CRCW08051R00FKEAHP
R4, R5, R27, R33, R38, R44, R49, R53, R58	9	Resistor	100k, 0.1W, 1%, 0603	Yageo	RC0603FR-07100KL
R7, R8	2	Resistor	1R , 0.1W, 1%, 0603	Yageo	RC0603FR-071RL
R9, R13, R29	3	Resistor	0 OHM, JUMPER, 1W, 1812	Yageo	RC1218JK-070RL
R10	1	Resistor	22R, 0.1W, 1%, 0603	Vishay	CRCW060322R0FKEAC
R11, R14, R78	3	Resistor	0 OHM, JUMPER, 0.1W, 0603_(DNP)	Panasonic	ERJ-3GEY0R00V
R12	1	Resistor	200k , 0.1W, 1% , 0603	Vishay	CRCW0603200KFKEA
R15	1	Resistor	30.1k, 0.1W, 1%, 0603	Vishay	CRCW060330K1FKEAC
R16, R17, R75	3	Resistor	1MEG, 0.1W, 1%, 0603	Vishay	CRCW06031M00FKEC
R18	1	Resistor	60.4k, 0.1W, 1% , 0603	Vishay	CRCW060360K4FKEAC
R19, R21, R118, R119	4	Resistor	100mR, 0.2W, 1%, 0603	Yageo	PT0603FR-7W0R1L
R20, R22, R76	3	Resistor	10mR, 1W, 1%, 1206	Vishay	WSLP1206R0100FEA
R23	1	Resistor	715k, 0.1W, 1% , 0603	Vishay	CRCW0603715KFKEA
R24, R63, R64, R65, R66, R67, R70, R100, R101, R102, R104, R108, R113, R126, R127, R128, R131	17	Resistor	1k, 0.1W, 1%, 0603	Panasonic	ERJ3EKF1001V

Reference	Qty	Type	Value/rating	Manufacturer	Part number
R26	1	Resistor	453k, 0.1W, 1% , 0603	Vishay	CRCW0603453KFKEA
R28	1	Resistor	49.9k, 0.1W, 0.1%, 0603	Panasonic	ERA-3AEB4992V
R30, R34, R40, R45, R51, R56	6	Resistor	1R , 0.1W, 1%, 0603	Yageo	RC0603FR-071RL
R31, R36, R41, R42, R47, R50, R54, R73	8	Resistor	10 OHM, 1% , 0.1W, 0603	Vishay	CRCW060310R0FKEA
R32, R37, R43, R48, R52, R57	6	Resistor	19.6 OHM, 1% , 0.1W, 0603	Vishay	CRCW060319R6FKEA
R35, R46, R55	3	Resistor	154k, 0.1W, 1%, 0603	Vishay	CRCW0603154KFKEA
R39, R59	DNP	Resistor	0 OHM ,JUMPER , 0.5W, 1210	Vishay	CRCW12100000Z0EA
R60, R61, R62, R68, R69, R71, R72, R74	8	Resistor	12k, 0.1W, 1%, 0603	Yageo	RC0603FR-0712KL
R79, R83, R85, R94, R95, R96, R97, R112	9	Resistor	0 OHM, JUMPER, 0.1W, 0603	Yageo	RC0603JR-070RL
R103	DNP	Resistor	0 OHM, JUMPER, 0.1W, 0603	Yageo	RC0603JR-070RL
R80	1	Resistor	10k, 0.1W, 1%, 0603	Yageo	RC0603FR-0710KL
R81, R86	DNP	Resistor	10k, 0.1W, 1%, 0603_(DNP)	Yageo	RC0603FR-0710KL
R82	1	Resistor	3.74K OHM, 1% , 0.1W, 0603	Vishay	CRCW06033K74FKEAC
R84	1	Resistor	6.2k, 0.1W, 1%, 0603	Yageo	RC0603FR-076K2L
R98, R99, R106, R107, R110, R111, R114	7	Resistor	100R, 0.1W, 1%, 0603	Panasonic	ERJ-3EKF1000V
R105	1	Potentiometer	10k, 0.5W, 10% , THT	Bourns	3362P-1-103T_LF
R109, R123, R124, R125, R139, R140	6	Resistor	4.87k, 0.1W, 1%, 0603	Vishay	CRCW06034K87FKEA
R120, R121, R122	3	Resistor	9.76k, 0.1W, 1% , 0603	Vishay	CRCW06039K76FKEA

Bill of materials

Reference	Qty	Type	Value/rating	Manufacturer	Part number
RS1, RS2, RS3	3	Resistor	0.002 OHM , 3W, 1% , 2512	Panasonic	ERJ-MS4SF2M0U
RT1	1	Sensor	SENSOR ANALOG, -40C-125C, SOT23-3	Microchip Technology	MCP9700T-E/TT
S1, S2	2	Slide Switch	SWITCH SLIDE SPST 0.4VA 28V	NKK Switches	AS11CP
U1	1	IC	BOY-II_PSC3_VQFN-48	Infineon Technologies	PSOC-C3-48PIN
S1, S2	2	Slide Switch	SWITCH SLIDE SPST 0.4VA 28V	NKK Switches	AS11CP
U1	1	IC	BOY-II_PSC3_VQFN-48	Infineon Technologies	PSOC-C3-48PIN
X9	1	Terminal Block	TERM BLK 5P SIDE ENT 2.54MM PCB	Phoenix Contact	1725685
ST1, ST2, ST3, ST4	4	Hex Standoff	HEX STANDOFF #4-40 ALUM 1-1/4"	Keystone Electronics	8407
HN1, HN2, HN3, HN4	4	Hex Nut	#4-40 Hex Nut 0.250" (6.35mm) 1/4"	B&F Fastener Supply	HNZ 440
P1,P2	2	Pin	ANCHOR PIN, THRU HOLE, 9mm	Alpha and Omega Semiconductors	ANCR-9
C1	1	Clip	HOOK PLATE, 24x24	Alpha and Omega Semiconductors	QSZ24x4

9 PCB layout

The REF_40VDC_1.5KW_SAW reference board utilizes a six-layer PCB with 2 oz copper for each layer. The multiple layers help dissipate heat when the board is running at high power. The dimensions are 3.1 inches/78.62 mm x 3.84 inches/97.11 mm with a width of 62 mils. The PCB meets certain standards such as the IPC. 600 Class 2 and 1AWIPC-RB-276 Class 1 standards. All pads on the board are solder mask defined and have an electroless nickel immersion gold (ENG) finish. FR-4 material is used for both the prepreg and core layers. Components are mounted on the top and bottom sides.

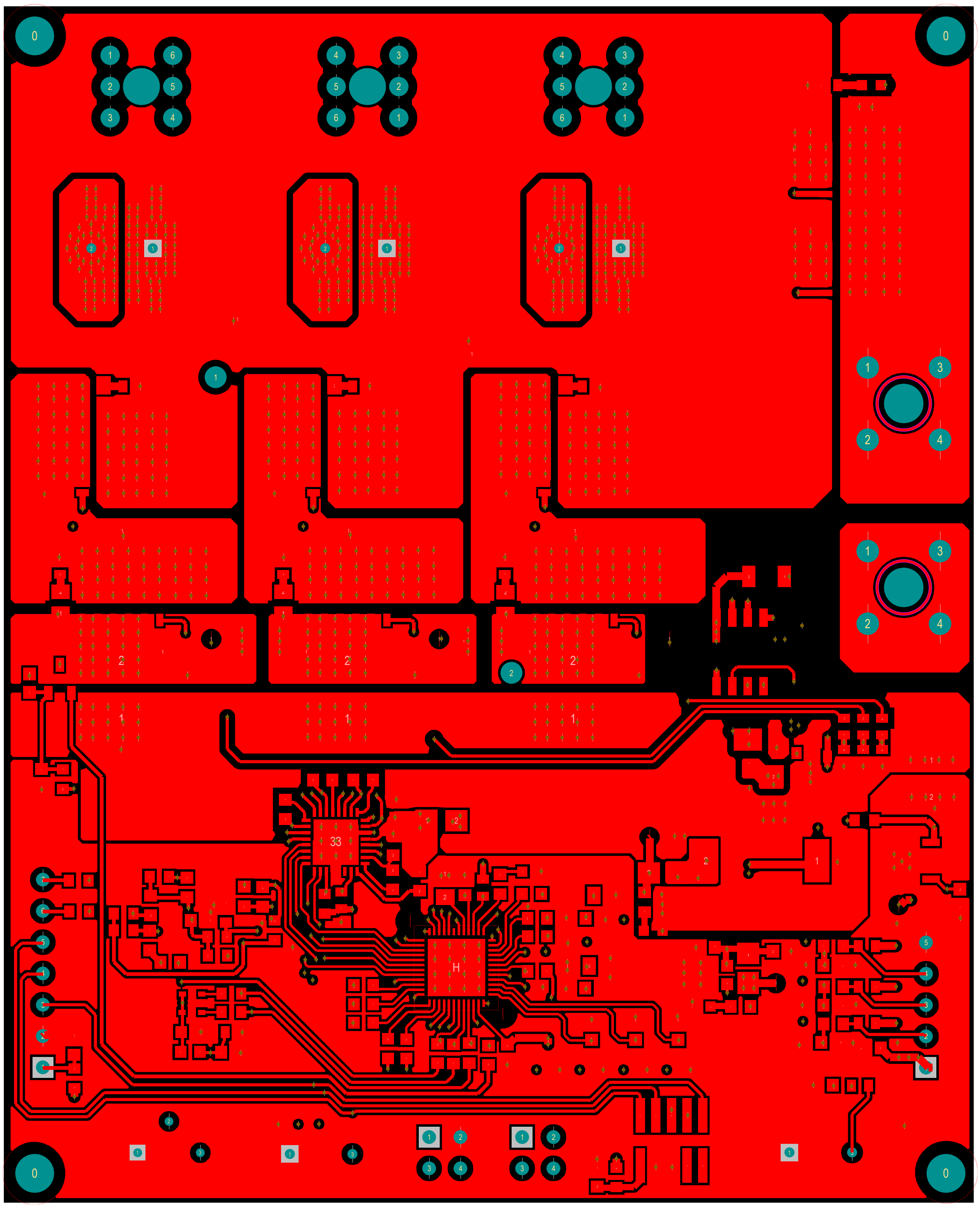

Figure 33 Top layer

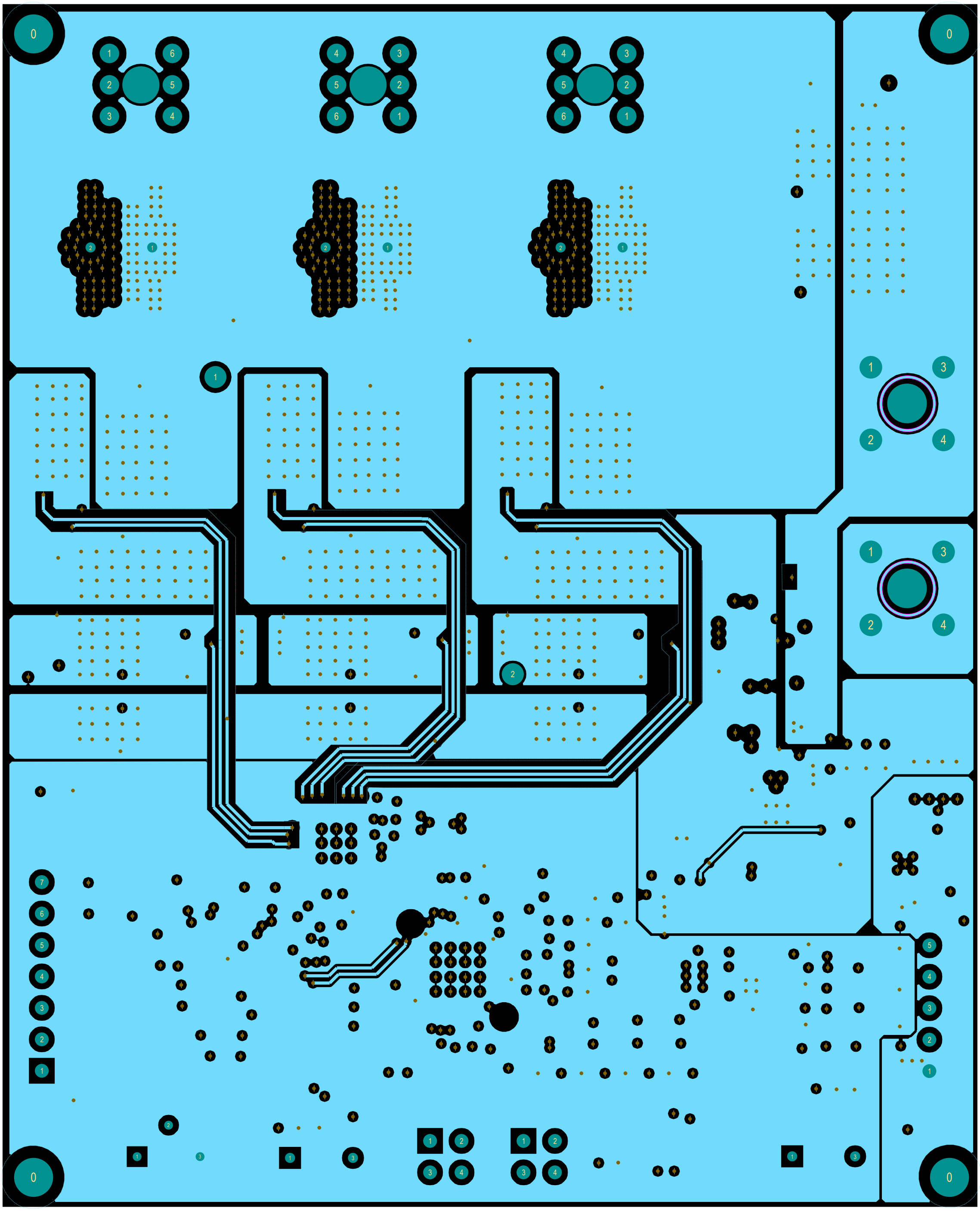

Figure 34 **Third middle layer**

The top and the middle third layers are designated power planes. The battery voltage, voltage input (V_{in}), and power ground are routed through the two layers via terminals (BATT+, PGND, and V_{in}). Both layers each have four nets and share three of those nets. The bottom polygon on each layer contains different nets. The bottom polygon on the top layer is designated for routing analog ground and the bottom polygon of the third middle layer used to route 3.3 V. The IC that require 3.3 V are placed on the bottom polygon. A 5 V polygon is implemented into the bottom-right of the third middle layer for Hall sensor usage. The top layer is used for carrying high current and routing components that require a higher input voltage, such as the electrolytic capacitors, shunts, and MOSFETs. Other signal layers are placed in between the power layers on purpose to enable effective heat dissipation.

As shown in Figure 9, electrolytic capacitors are placed close to the battery terminals in order to filter out unwanted noise and high ripple. The MOSFETs are also placed close to the battery terminals to minimize parasitic inductance. This reduces voltage drops and creates a smaller loop area for the current path.

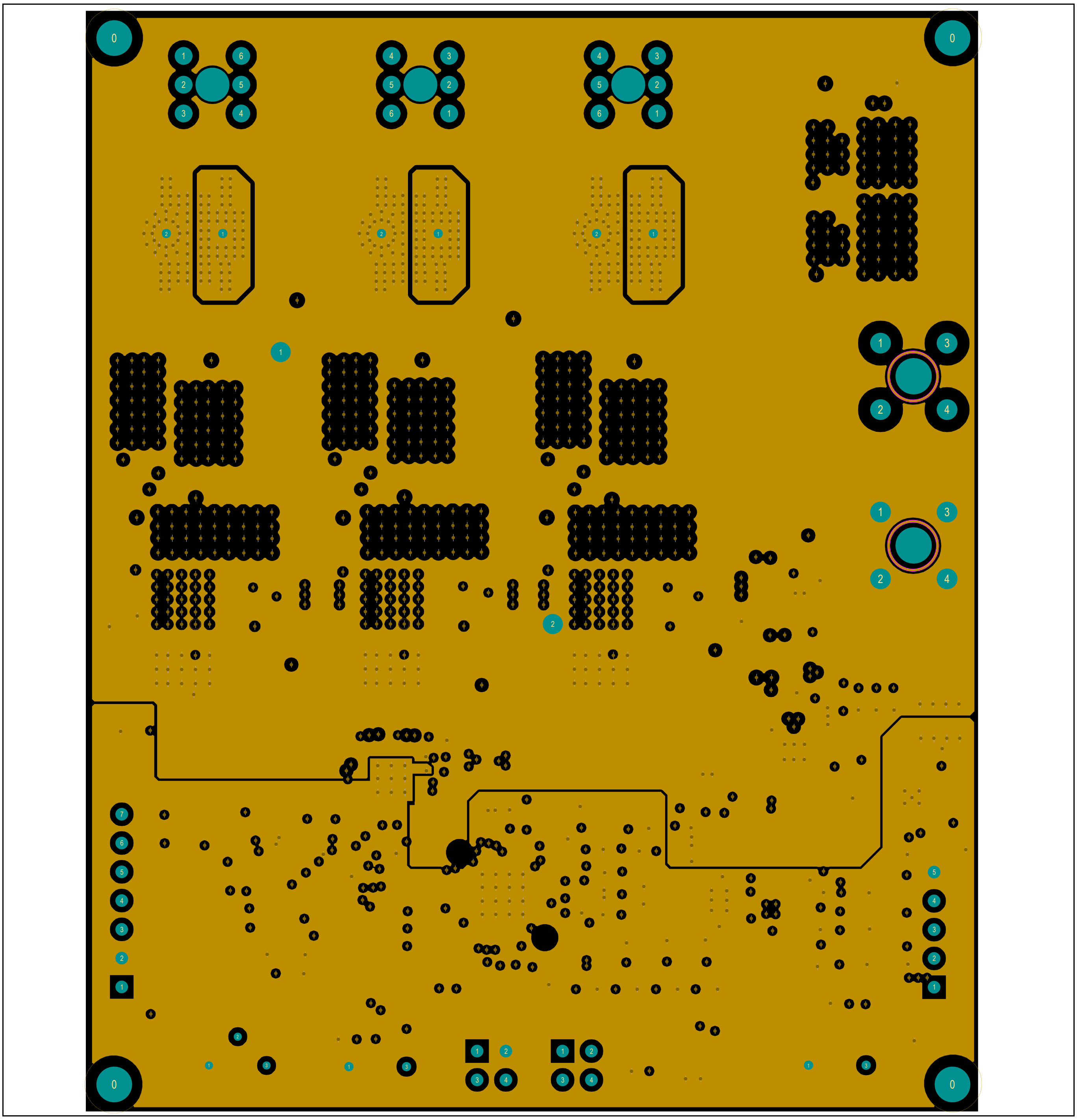

Figure 35 **First middle layer**

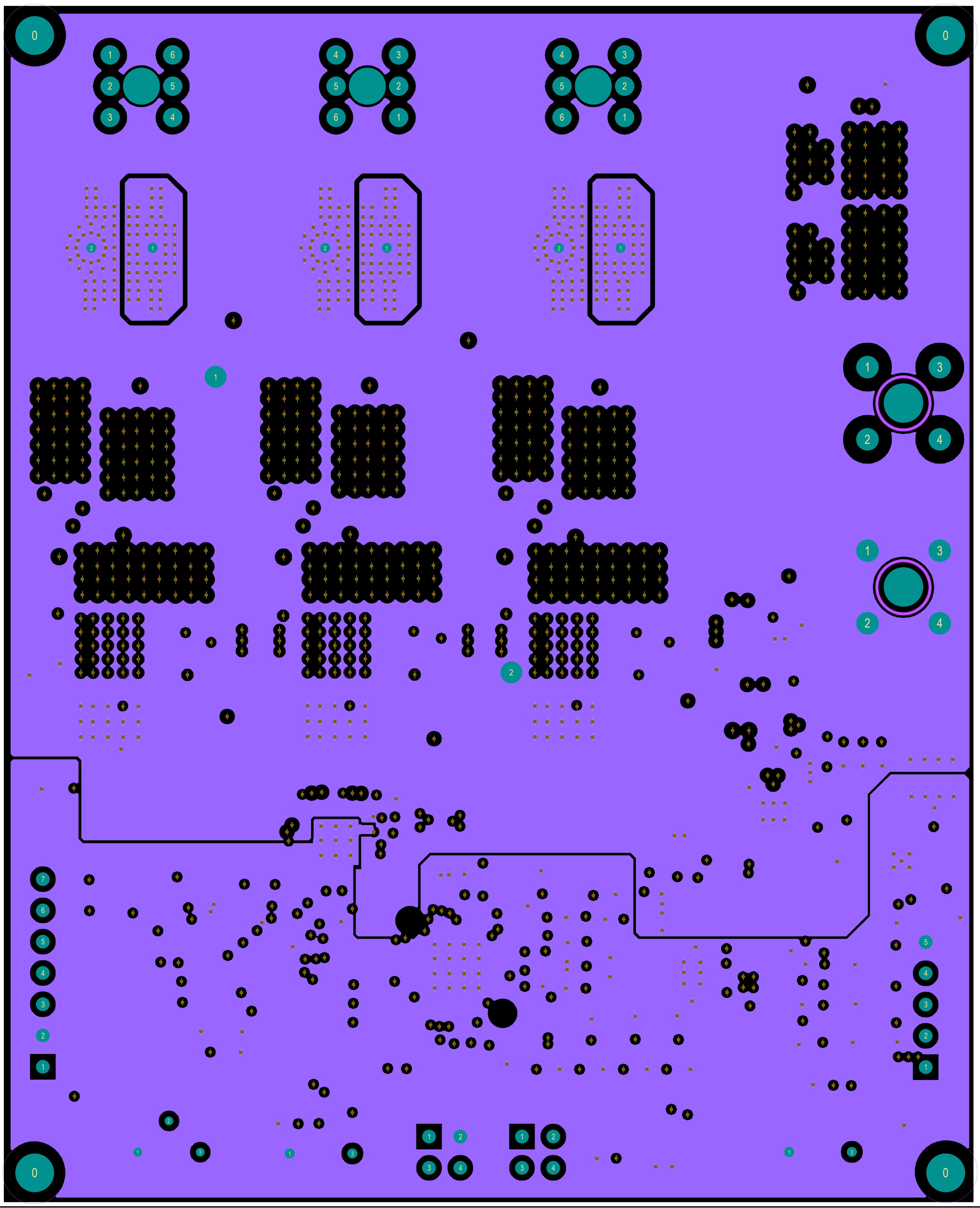

Figure 36 **Fourth middle layer**

The first and fourth middle layers are designated ground planes that are shorted out via R29. The top portion of both the layers is designated for power ground and the bottom portion below the shunts is designated for analog ground. These two ground planes provide a common reference point for electrical signals and provide a return path for currents. The ground planes are placed in between the signal/power planes to avoid introducing new or relying on existing decoupling capacitors to mitigate EMI problems. The fourth middle layer is not only utilized for ground nets but also contains V_{in} polygons. The components carrying high current are placed on the top half of the board to minimize EMI interference and provide a low-impedance return path for the currents. As mentioned before, the bottom portions of both the layers are reserved for analog signals and grounding. ICs that require less current are placed in the bottom portion to minimize high impedance and parasitic.

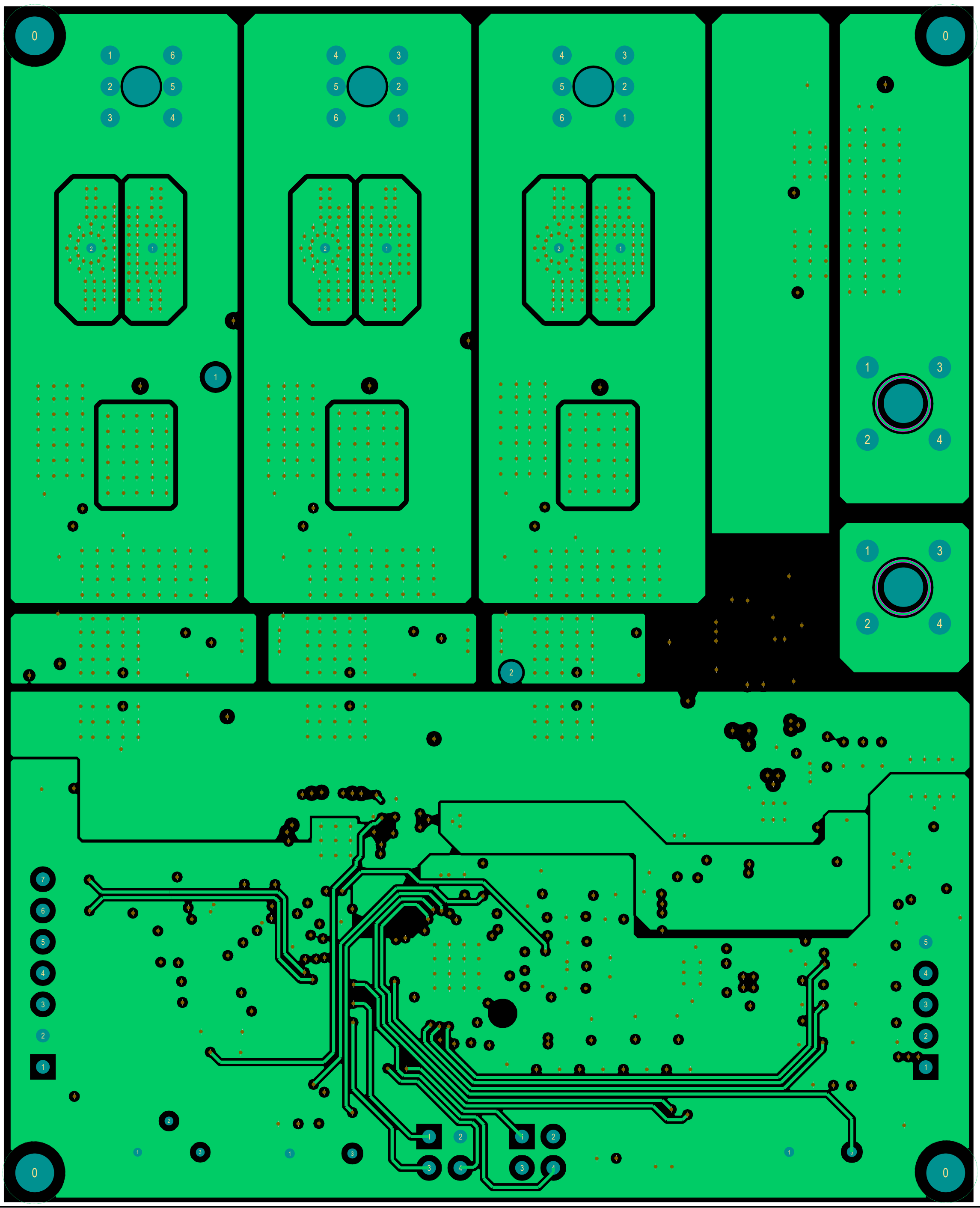

Figure 37 **Second middle layer**

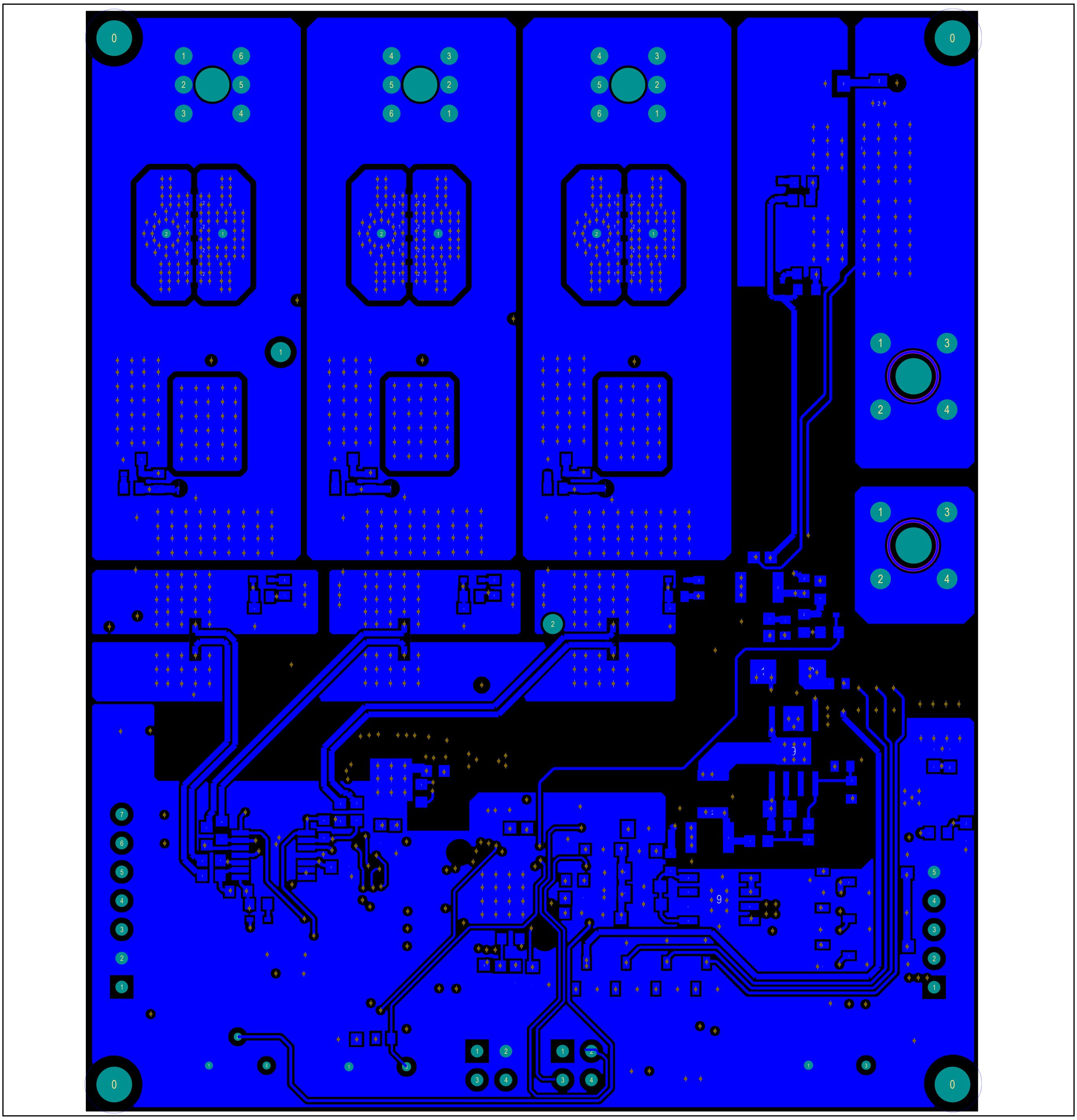

Figure 38 Bottom layer

The second middle layer and bottom are used for phase connections. Both layers contain large polygons that support high current to flow through the phases, shunts, and MOSFETs. As shown in Figures 37 and 38, each phase has a significant amount of vias placed where the electrolytic capacitors, MOSFETs, and shunts sit. These vias help thermal conductivity between the components and different PCB layers, letting heat dissipate at a faster rate.

2 A large polygon runs from the top of the phase terminals to the high side of the three-phase inverter while another polygon runs from the low side of the inverter to the shunts. Both layers support the same nets, however, the second middle layer contains a polygon with a 12 V net used to route ICs that require 12 V.

10 Test results

10.1 Power measurements

The power measurements were observed using a power analyzer. Current transducers were connected on each phase of the motor and the battery voltage was sensed directly from the board terminals. The results below were captured once steady state was reached while the motor was running with 2 N·m of torque. The first column to the very left of Figure 39 shows the output voltage (V_{RMS}) of each phase and the battery voltage (39.6278 V). The second column to the left shows the I_{RMS} currents of each phase and the DC input current (26.9960 A). The third column the output power of the inverter (1.04974 kW) and the column to the very right displays its efficiency.

The input power is measured to be: 39.6278 V × 26.9960 A = 1.06978 kW

Therefore, the efficiency = $1.04974\ \mathrm{kW}/1.06978\ \mathrm{kW}$ = 98.127%

Figure 39 Inverter efficiency (continuous)

10.2 Thermal measurements

The thermal images below were captured once the board reached stead-state under the following conditions:

- No air flow/fan
- Motor speed of 4077 rpm
- 2.0 N·m load

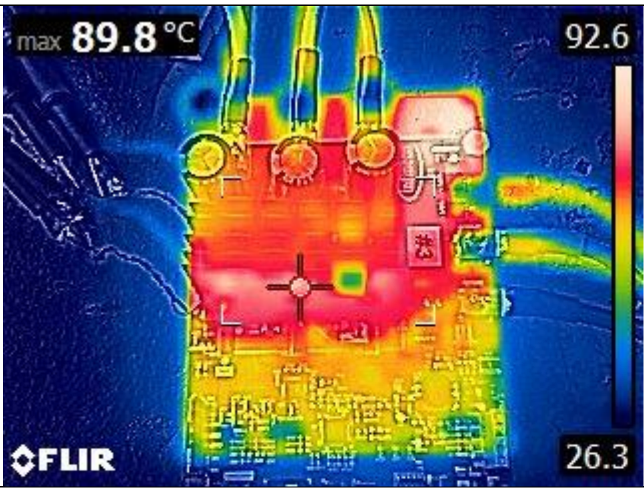

Figure 40 Thermal Measurement, 89.8 °C

The thermal camera captured the image in such a way that the cursor would automatically pinpoint the area of the board that had the highest temperature**.** The hottest area of the board is located on the shunt of the middle phase (V_{phase}). A higher amount of current is sensed in the middle phase, causing the shunt on V_{PHASE} to be higher in temperature. The shunt reached a maximum of 90.1°C and a minimum of 89.8°C at steady-state while maintaining an efficiency of ~98.0%. The MOSFET's temperature could not be directly monitored due to the heatsink.

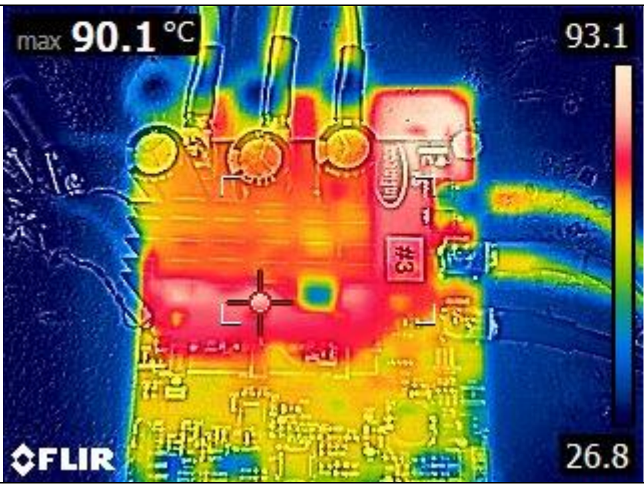

Figure 41 Thermal Measurement, 90.1 °C

Note: The shunt's reflection on the thermal camera shifted the image upward, creating the illusion that the source of the low-side MOSFET on V_{PHASE} is the hottest part of the board.

10.3 Operating waveforms

The following waveforms show the phase currents and the drain-to-source voltage (V_{DS}) on phase U (U_{PHASE}). The waveforms were captured at steady-state with an output power of 1 kW. In addition, the motor was running at a speed of 4077 rpm with a load of 2 N·m. The drain-to-source voltages on U_{PHASE} was observed to show the worst-case scenario. This phase is considered the worst-case due to the position of the phase being the furthest from the battery voltage (Figure 42). V_{DS_LS} reached a maximum voltage of 40 V_{PK-PK} and V_{DS_LS} reached a maximum voltage of 40.4 V_{PK-PK}. Both switching voltage readings remained well under 20% of the voltage rating. Little to no transient can be seen on the switching waveforms due to the snubbers across the drain to source terminals.

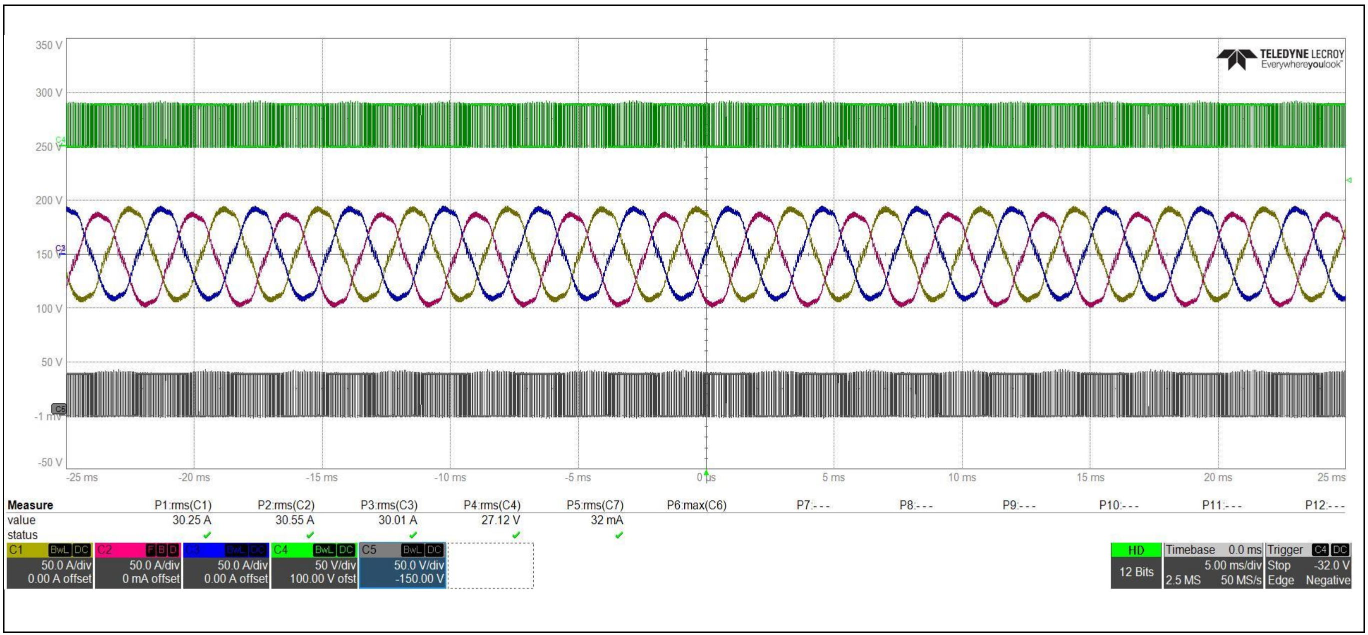

Figure 42 Phase currents and U phase V_{DS} waveforms, $V_{DS\_LS\_phU}$ (Ch4), $V_{DS\_HS\_phU}$ (Ch5), I_{phase_U} (Ch1), I_{phase_V} (Ch2), I_{phase_W} (Ch3)

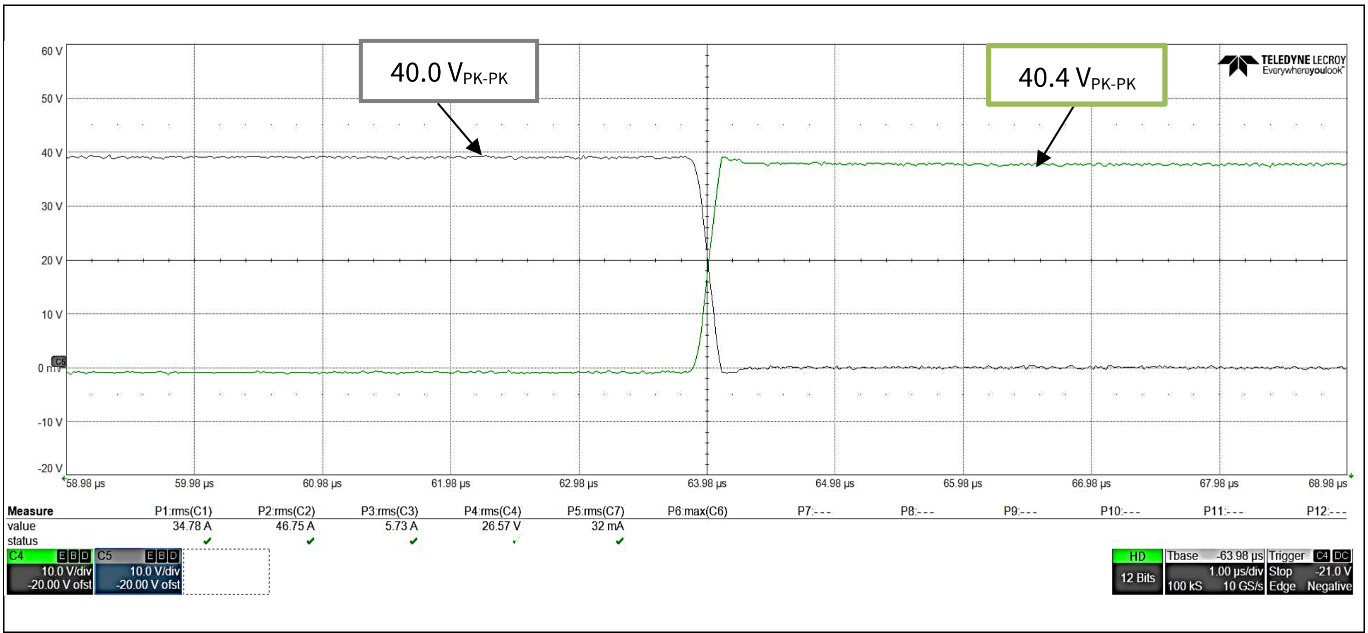

Figure 43 U phase V_{DS} waveforms, $V_{DS\_LS\_phU}$ (Ch4), $V_{DS\_HS\_phU}$ (Ch5)

The phase currents ranged as low as 29.79 A_{RMS} and as high as 30.5 A_{RMS} (Figure 44). The waveforms remained balanced while the motor was running at 4077 rmp with a load of 2.0 N·m.

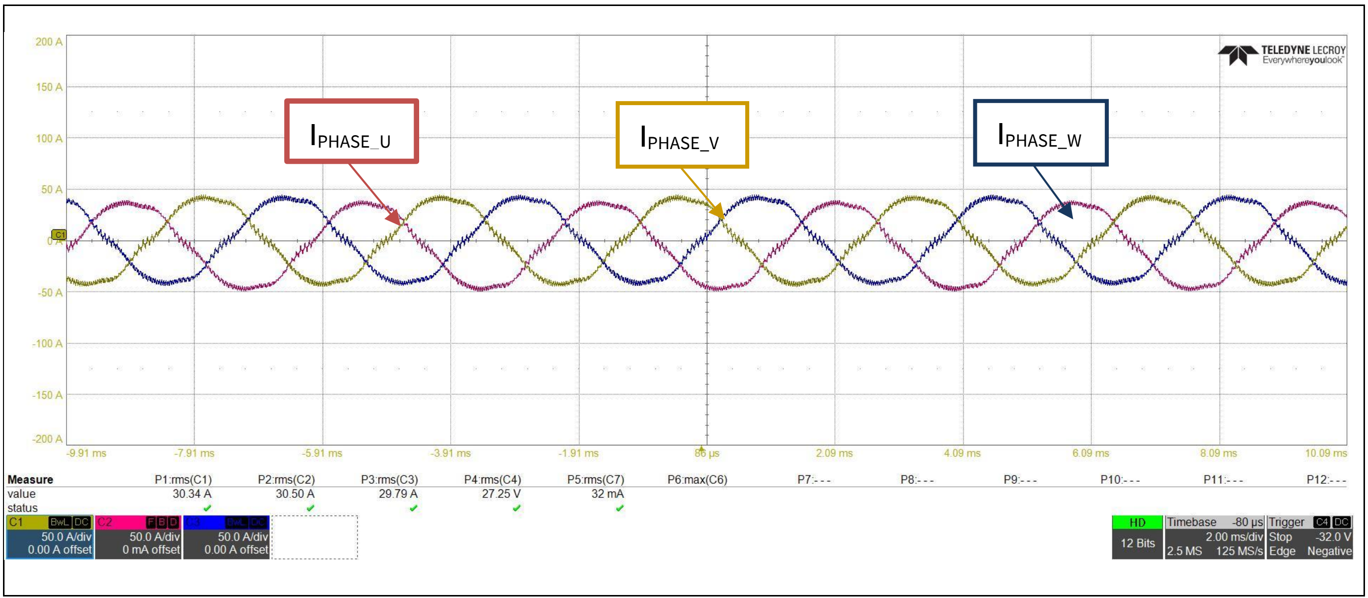

Figure 44 **Phase currents at 2.0 N·m and 4077 rmp, I_{phase_U} (Ch1), I_{phase_V} (Ch2), I_{phase_W} (Ch3)**

11 Summary

The reference board meets requirements and specifications required in power tools or three-phase motor designs. The hardware of the board has been discussed, such as its circuitry and PCB layout. Infineon's 1EDL8011 and 6ED2742S01Q have been highlighted in the application note. It has been explained how both ICs provide a solution for motor control solutions. Infineon's IQFH61N06NM5 has proven to be a reliable solution for motor drive applications due to its superior thermal resistance and very low on-resistance. Each layer of the PCB has been explained in this application note. The board was laid out in a way that allows optimal thermal dissipation, reduces parasitic, and provides high current paths. The operation of the board has also been covered in detail from test setup to execution.

The GUI gives you the freedom to customize parameters and select different FOC options. You also have the ability to customize firmware and configure parameters to any motor. The motor tuning feature has proven to be a useful tool that eliminates unnecessary component modifications. This feature simplifies the product development process and reduces time-to-market. Data, graphs and waveforms can be seen and accessed through the GUI. Other features such as the test bench lets you test or run systems using motors without costly equipment such as an oscilloscope or power analyzer.

The firmware has been verified through testing. The FOC control algorithm has also been described, including the methods for entering the motor parameters and tuning the control loops using ModusToolbox™. The test results show that Andromeda is effective in important areas such as speed control, phase advance, MPTA, flux weakening, MTPV, and current controlling. Mathematical models have been shown and used to explain how andromeda is implemented. The equations and algorithms for these areas have been explained in this application note.

The reference board has proven to operate under high load conditions while maintaining an efficiency of about 98%. The board can support up to 1.5 kW with no additional cooling and can operate at a steady state without any area of the board exceeding a temperature of 95°C. Despite the waveforms being captured on the U phase showing the worst-case scenario, the current waveforms were balanced with little ripple through high-speed testing (4077 rpm) and high torque testing (2 N·m). The voltage readings remained well under 20% of the voltage rating. Little to no transient was seen on the switching waveforms due to the snubbers across the drain to source terminals. The REF_40VDC_1.5KW_SAW has proven to be an efficient solution for motor control applications.

References

[1] Infineon Technologies AG: *Motor Handbook (Version 2.1)*; Available online

[2] Infineon Technologies AG: Application note – *Sensorless Field Oriented Control with Embedded Power SoC*; Available online

[3] Infineon Technologies AG: Application note – *Block commutation vs. FOC in power tool motor control*; Available online

[4] Infineon Technologies AG: Application note – *PMSM FOC motor control software using XMC™*; Available online

[5] Infineon Technologies AG: Whitepaper – *Power Loss and Optimized MOSFET Selection in BLDC Motor Inverter Designs – Understanding MOSFET power losses in block (trapezoidal) commutation*; Available online

[6] Zhang, Wei-Feng Zhang/ Yu, Yue-Hui: *Comparison of Three SVPWM Strategies* – Journal of Electronic Science and Technology of China (Vol. 5, No. 3) – 2007-09

[7] MAGTROL: *Hdseries - Hysteresis Dynamometers*; Available online

[8] Cadence PCB Solutions: Thermal Vias for Circuit Board Heat Management: Techniques and Tips, Cadence, [Online]; Available online

[9] MacroFab: *Via in Pad PCB Design* – March 20, 2019; Available online

[10] AdvancedPCB: *The Importance of Power and Ground Planes in PCB Design* – 8-15-2024; Available online

Register your Infineon evaluation board, reference design or demo kit board

When receiving your order, you are only three steps away from unlocking what Infineon's application engineers have prepared for you as the new owner of a very specific Infineon evaluation board, reference design or demo kit: Product registration

Revision history

Document version	Date of release	Description of changes
V 1.0	2025-04-22	Initial release

Trademarks
All referenced product or service names and trademarks are the property of their respective owners.
PSOC™, formerly known as PSoC™, is a trademark of Infineon Technologies. Any references to PSoC™ in this document or others shall be deemed to refer to PSOC™.

Edition 2025-04-22

Published by

Infineon Technologies AG

81726 Munich, Germany

Do you have a question about this document?

Email: erratum@infineon.com

Document reference

Important notice
The information contained in this application note is given as a hint for the implementation of the product only and shall in no event be regarded as a description or warranty of a certain functionality, condition or quality of the product. Before implementation of the product, the recipient of this application note must verify any function and other technical information given herein in the real application. Infineon Technologies hereby disclaims any and all warranties and liabilities of any kind (including without limitation warranties of non-infringement of intellectual property rights of any third party) with respect to any and all information given in this application note.

The data contained in this document is exclusively intended for technically trained staff. It is the responsibility of customer's technical departments to evaluate the suitability of the product for the intended application and the completeness of the product information given in this document with respect to such application.

Warnings
Due to technical requirements products may contain dangerous substances. For information on the types in question please contact your nearest Infineon Technologies office.

Except as otherwise explicitly approved by Infineon Technologies in a written document signed by authorized representatives of Infineon Technologies, Infineon Technologies' products may not be used in any applications where a failure of the product or any consequences of the use thereof can reasonably be expected to result in personal injury.